

Functional and Evolutionary Analysis of Flatfish Gonadotropin Receptors Reveals Cladal- and Lineage-Level Divergence of the Teleost Glycoprotein Receptor Family¹

François Chauvigné,⁴ Angèle Tingaud-Sequeira,^{4,5} María J. Agulleiro,^{4,6} Magdalena Calusinska,^{4,7} Ana Gómez,⁶ Roderick Nigel Finn,^{3,8} and Joan Cerdà^{2,4}

Laboratory of Institut de Recerca i Tecnologia Agroalimentàries (IRTA)-Institut de Ciències del Mar,⁴
Consejo Superior de Investigaciones Científicas (CSIC), Barcelona, Spain

Génomique et Physiologie des Poissons,⁵ Talence, France

Department of Fish Physiology and Biotechnology,⁶ Instituto de Acuicultura Torre de la Sal, CSIC, Castellón, Spain

Centre for Protein Engineering,⁷ University of Liège, Liège, Belgium

Department of Biology,⁸ University of Bergen, Bergen High Technology Center, Bergen, Norway

ABSTRACT

Pituitary gonadotropins, follicle-stimulating hormone (FSH), and luteinizing hormone (LH) act via their cognate glycoprotein hormone receptors (GpHRs), FSH receptor (FSHR), and LH/choriogonadotropin receptor (LHCGR) to regulate gonad physiology. Here, we show that the flatfish Senegalese sole (*Solea senegalensis*) expresses functional isoforms of *fshr* and *lhcr*, but the genomic origin, ligand activation, and tissue distribution of the receptor transcripts are more complex than expected. By integrating the molecular phylogeny of GpHRs with the syntenic loci of vertebrate orthologs, and by subsequently characterizing the physical maps with the phylogeny of flanking genes, we found that vertebrate GpHRs have undergone a divergent evolution. In Teleostei, *fshr* genes have a common descent and can be classified as *fshra*, whereas *lhcr* genes exist as alternatively coded genes even in closely related species. Structural analyses of the receptors revealed that *Fshra* has an elongated ligand-binding domain, containing an extra leucine-rich repeat that specifically arose in the Acanthomorpha because of exon duplication. Ectopic expression in *Xenopus laevis* oocytes demonstrated that sole *Fshra* responded to piscine Fsh and Lh, whereas *Lhcrba* was preferentially activated by its cognate hormone. The expression pattern of sole *fshra* and *lhcrba* in gonads during the reproductive cycle was consistent with earlier observations wherein *Fshra* regulates ovarian growth and spermatogenesis and *Lhcrb* triggers gamete maturation, respectively. However, contrary to observations in other teleosts, *fshra* was localized exclusively in Sertoli cells of the testis, whereas *Lhcrba* was expressed in Leydig cells as well

as in spermatids. These results demonstrate the presence of alternatively coded *lhcr* isoforms (*lhcrba* and *lhcrbb*) in teleosts and suggest a role of the *lhcrba* receptor in the differentiation of spermatids into spermatozoa in Senegalese sole.

evolution, follicle-stimulating hormone receptor, *Fshr*, gametogenesis, gene conversion, gonadotropin, *Lhcr*, luteinizing hormone, ovary, spermatid, spermatogenesis, teleosts

INTRODUCTION

In vertebrates, the brain-pituitary-gonad axis carries out the hormonal control of reproduction. Among other pituitary hormones, the gonadotropins follicle-stimulating hormone (FSH) and luteinizing hormone (LH) are key regulators of germ cell development in both males and females [1]. These circulating glycoproteins are heterodimers composed of one common glycoprotein α subunit (CGA) and one hormone-specific β subunit (FSHB and LHB) [2]. The duality of the LH/FSH signaling system is conserved throughout vertebrates [3], and it is assumed that duplication of an ancestral gene in Agnatha gave rise to LH and FSH in the jawed vertebrates (Gnathostomata) [4]. In Teleostei, the presence of two gonadotropins (GTH I and GTH II) was first documented for salmonids [5]. Subsequent investigations have revealed the homologous nature of the gonadotropins between Teleostei and Mammalia, such that GTH I and GTH II are now termed Fsh and Lh, respectively [6, 7]. Consequently, it is thought that in teleosts, as in mammals, Fsh regulates early gametogenesis and gonad development, whereas Lh triggers meiotic maturation of gametes followed by spermiation or ovulation [8–12].

The gonadotropins exert their action on reproductive tissues via their cognate receptors, the LH/choriogonadotropin receptor (LHCGR) and the FSH receptor (FSHR), each members of the family of glycoprotein hormone receptors (GpHRs). In Teleostei, cDNAs encoding two distinct gonadotropin receptors, *Fshr* and *Lhcr*, have been identified within a broad range of species, including members of the Elopomorpha [13], Ostariophysii [14–18], Protacanthopterygii [19–23], Paracanthopterygii [24], and Acanthopterygii [25–28]. In each case, the overall structural homology to mammalian counterparts was conserved. These G protein-coupled receptors consist of a large extracellular domain, characterized by multiple leucine-rich repeats (LRRs) that are critical for specific hormone binding, a seven-transmembrane domain (7TMD), and a short intracellular C-terminus [29]. In Mammalia, the affinity of each gonadotropin for its receptor is highly specific, but in Teleostei,

¹Supported by Genome Spain and Genome Canada within the framework of the international consortium Pleurogene (to J.C.) and by a grant from the Research Council of Norway (178837/40 to R.N.F.). F.C. was supported by a postdoctoral fellowship from Juan de la Cierva Programme (Spanish Ministry of Education and Science). M.J.A. was supported by a predoctoral fellowship from the Instituto Nacional de Investigación y Tecnología Agraria y Alimentaria (INIA, Spain) and later by the Juan de la Cierva Programme.

²Correspondence: Joan Cerdà, Lab IRTA-Institut de Ciències del Mar (CSIC), Passeig marítim 37-49, 08003 Barcelona, Spain. FAX: 34 93 230 95 55; e-mail: joan.cerda@irta.cat

³Correspondence: Roderick N. Finn, Department of Biology, University of Bergen, Bergen High Technology Centre, Postboks 7803, N-5020 Bergen, Norway. FAX: 47 55 589667; e-mail: nigel.finn@bio.uib.no

Received: 30 October 2009.

First decision: 9 January 2010.

Accepted: 15 February 2010.

© 2010 by the Society for the Study of Reproduction, Inc.

eISSN: 1529-7268 <http://www.biolreprod.org>

ISSN: 0006-3363

Fshr and Lhcgr can be cross-activated by their ligands and, therefore, receptor specificity is yet unclear [7, 30].

In mammalian and avian species, the expression pattern and function of gonadotropin receptors are mutually exclusive. FSHR regulates the proliferation and function of Sertoli cells in the testis [31] and of granulosa cells in the ovary, whereas LHCGR activates steroidogenesis in testicular Leydig cells and in theca and granulosa cells [32–34]. In Teleostei, however, this segregation seems less evident. In the teleost ovary, Fshr and Lhcgr are expressed in the ovarian granulosa and theca cells surrounding the oocyte [35, 36]. Both of these follicular layers have steroidogenic functions for the production of estrogens or progestogens during oocyte growth and maturation, respectively [36]. By contrast, Fshr in Sertoli cells is believed to mediate the proliferation of spermatogonia through the synthesis and release of growth factors, whereas the Lhcgr in Leydig cells is involved in steroid production [37, 38]. However, in some physiological situations, such as at the onset of spermatogenesis and during rapid testicular growth, Fsh may show prominent androgenic potency (i.e., testosterone and 11-ketotestosterone production [37, 39, 40]), which may be mediated through the activation of Fshr expressed in Leydig cells [40, 41]. Nevertheless, current knowledge regarding the physiological functions of Fshr and Lhcgr in fish gonads is based on a few species of salmonids, eels, cyprinids, and catfishes. Therefore, information about the evolution and physiology of Fshr and Lhcgr in more advanced teleosts, such as Pleuronectiformes (flatfishes), may contribute novel information regarding the biological role of these receptors.

We have previously isolated and characterized the cDNAs encoding the β subunits of Fsh and Lh, as well as the common Cga subunit, of the flatfish Senegalese sole (*Solea senegalensis*) and found that their expression pattern in the pituitary implied that these hormones may regulate spermatogenesis in the semicyclic, asynchronous testis of this species [42]. To further investigate this mechanism, in the present study we have isolated the Senegalese sole gonadotropin receptors, characterized their functional activity, and examined their transcriptional expression in adult tissues and in gonads during the reproductive cycle. After initially examining the phylogeny of the cloned receptors, we noted that the Senegalese sole *lhcgr* did not cluster as a typical pleuronectiform receptor. Consequently, we carried out extensive phylogenetic and syntenic analyses, which revealed that whereas Teleostei appear to encode singular variants of the *fshr* and *lhcgr* genes, their origins are equivocal. The data suggest that *fshr* evolved from a common ancestor at the root of the crown clade. Conversely, teleost *lhcgr* genes seem to have experienced a complex history whereby two mutually exclusive genes exist within the lineage, but their functions have mostly converged.

MATERIALS AND METHODS

Animals and Sampling

The adult Senegalese sole F_1 generation was raised as previously described [43]. Males used in the present study were maintained under controlled temperature during winter so that the temperature was less than 10°C for approximately 3 wk [44]. Females ($n = 5$ –6; weight, 1290 ± 40 g, mean \pm SEM) and males ($n = 10$; weight, 730 ± 35 g, mean \pm SEM) were killed at times that corresponded to different folliculogenic/spermatogenic stages as determined by histological examination of gonads. To obtain females with maturing and mature ovaries, fish were collected in May and treated with an intramuscular injection of 5 μ g/kg of gonadotropin-releasing hormone agonist [D-Ala⁶, Pro⁹, NEt] (GnRHa) and sampled 24–48 h later as previously described [43]. At all sampling times, fish were sedated with 500 ppm of phenoxyethanol and killed by decapitation. One piece of the gonad

was deep-frozen in liquid nitrogen and stored at -80°C until RNA extraction. Two additional pieces of the gonad adjacent to the piece sampled for RNA extraction were fixed in modified Bouin solution (75% picric acid and 25% formalin) for histological analysis or in 4% paraformaldehyde for in situ hybridization. Procedures relating to the care and use of animals were approved by the Ethics Committee from Institut de Recerca i Tecnologia Agroalimentàries (IRTA, Spain) in accordance with the Guiding Principles for the Care and Use of Laboratory Animals.

Isolation of Ovarian Follicles

Subsamples of the ovaries were immediately removed and placed in Petri dishes (diameter, 60 mm) containing 10 ml of 75% Leibovitz L-15 medium with L-glutamine (Sigma) and 100 mg/ml of gentamicin (pH 7.5) [45]. Follicle-enclosed oocytes at previtellogenesis, early vitellogenesis, vitellogenesis, maturation, and atresia were isolated manually using watchmaker forceps under a stereomicroscope. Follicle samples were frozen in liquid nitrogen and stored at -80°C .

Histological Analysis

Ovaries and testes were fixed in Bouin solution for 3–4 h, dehydrated, embedded in paraplast, sectioned (thickness, 5 μ m), and stained with hematoxylin-eosin. The relative fractions of previtellogenic, early vitellogenic, vitellogenic, mature, and atretic ovarian follicles were calculated by counting 100–150 total ovarian follicles in at least three different histological sections from the same ovary as described previously [43]. The fractional prevalence of spermatogonia A (SgA), spermatogonia B (SgB), spermatocytes (Sp), spermatids (Spd), and spermatozoa (Spz) in testes were scored on at least five different seminiferous lobules in five different histological sections per fish as described by Agulleiro et al. [44].

Cloning of Senegalese Sole *fshr* and *lhcgr* cDNAs

Total RNA was extracted from testes using the RNeasy mini kit (Qiagen) and treated with DNase using the RNase-Free DNase kit (Qiagen) following the manufacturer's instructions. An aliquot of 10 μ g of total RNA was reverse transcribed using 20 IU of AMV RT (Stratagene), 0.5 μ M oligo(dT)_{12–18} (Invitrogen), 40 IU of RNase inhibitor (Roche), and 1 mM dNTPs for 1.5 h at 50°C. The PCR was carried out with 0.5 μ l of the RT reaction in a volume of 50 μ l containing 1 μ l of PCR buffer plus Mg²⁺, 0.2 mM dNTPs, 10 μ M of each forward and reverse oligonucleotide primers, and 1 IU of Taq polymerase (Roche). Degenerate forward and reverse primers were designed for conserved nucleotide regions among teleost *fshr* and *lhcgr* cDNAs available in public databases (Supplemental Table S1; all Supplemental Data are available online at www.biolreprod.org). Reactions were amplified using one cycle of 95°C for 5 min, then 40 cycles of 95°C for 1 min, 55°C for 1 min, and 72°C for 2 min, followed by a final 7-min elongation at 72°C. The products were cloned into the pGEM-T Easy Vector (Promega) and sequenced by BigDye Terminator Version 3.1 cycle sequencing on ABI PRISM 377 DNA analyzer (Applied Biosystems). Full-length sole *fshr* and *lhcgr* cDNAs were isolated by rapid amplification of cDNA ends (RACE; Gibco) followed by a final amplification with a high-fidelity polymerase (EasyA; Stratagene). Full-length cDNAs were sequenced as stated above. The nucleotide sequence of Senegalese sole *fshra* and *lhcgrba* have been deposited in the GenBank database under accession numbers GQ472139 and GQ472140, respectively.

Structural, Phylogenetic, and Syntenic Analyses

To ascertain the salient structural features of the Senegalese sole gonadotropin receptors, the transcripts were compared to genomic orthologs in other teleosts (www.ensembl.org), whereas the deduced amino acid sequences were analyzed in silico using Pfam [46], SignalP 3.0 [47], NetNGlyc 1.0 (www.cbs.dtu.dk/services/NetNGlyc), and TMHMM v. 2.0 [48] and modeled against the crystallographically resolved structure for human FSHR [49] using Cn3D [50]. Molecular phylogenies of amino acid and codon (triplet nucleotide) alignments were determined as described by Finn and Kristoffersen [51]. Orthologs of *fshr*, *lhcgr*, and their related thyroid-stimulating hormone receptors (*tshr*) were obtained from public databases, and alignments were constructed using the T-Coffee suite of tools [52]. Tree topologies were established using Bayesian (Mr Bayes Version 3.1.2) and maximum likelihood (ML; PAUP Version 10b) methods of phylogenetic inference [53]. For Bayesian analyses, the following settings were used for codon alignments: nucmodel = 4by4, nst = 2, rates = gamma. The settings for amino acid

alignments were: aamodel = mixed, with 1 000 000 generations, sampled every 100 generations using four chains and a burnin of 3500. For each run, a majority-rule consensus tree together with posterior probabilities for the last 6500 trees, representing 650 000 generations was arranged using Arceopteryx [54] and subsequently rendered with Geneious Pro (Biomatters Ltd.).

To validate the tree topologies, reconstruction of the *fshr*, *lhcr*, and *tshr* linkage maps was achieved using ensembl (v56) and the Genomicus genome browser (v56.01; www.dyogen.ens.fr). Two methods of reconstruction (alignment and phylogeny) were used to evaluate the evolutionary heritage of these submembers of the LRR receptor superfamily. The physical maps, gene loci, and nomenclature were annotated using ensembl. Because the tree topologies indicated that two *lhcr* genes (*lhcrba* and *lhcrbb*) exist within the teleost crown clade, we conducted additional phylogenetic analyses (Bayesian and ML) of the duplicated neurexin (*nrxn*) genes that immediately flank the *fshr*, *lhcr*, and *tshr* loci. These latter analyses provided an independent means of validating the nomenclature for teleost gonadotropin receptors proposed in the present work.

Expression of Senegalese Sole *Fshra* and *Lhcrba* in *Xenopus laevis* Oocytes

Senegalese sole *fshra* and *lhcrba* constructs for heterologous expression in *Xenopus laevis* oocytes were generated by subcloning the corresponding full-length cDNAs into the pT7Ts expression vector [55]. Because this vector contains unique *EcoRV* and *SpeI* cloning sites to allow the gene of interest to be flanked by the 5' and 3' untranslated regions of the *X. laevis* β -globin gene, compatible *EcoRV* and *SpeI* sites were introduced in the sole *lhcrba* cDNA by PCR. For *fshra*, only *SpeI* sites were added, because the sequence contains an internal *EcoRV* site, and the orientation was checked after ligation by restriction profile. For both receptors, the FLAG tag sequence (N-DYKDDDDK-C) was introduced by PCR after the C-terminus of the encoded protein, just before the stop codon, to monitor protein translation by immunocytochemistry. Capped RNA (cRNA) for microinjection was synthesized with T7 RNA polymerase from *Sall*-linearized pT7Ts-*fshra*-FLAG or pT7Ts-*lhcrba*-FLAG constructs. Isolation of stages V and VI oocytes and microinjection of cRNA was performed in MBS (modified Barth's medium: 88 mM NaCl, 1 mM KCl, 2.4 mM NaHCO₃, 0.82 mM MgSO₄, 0.41 mM CaCl₂, 0.33 mM Ca(NO₃)₂, 10 mM Hepes [pH 7.5], and 48 mg/L of gentamicin) as previously described [55]. After microinjection, manual defolliculation was carried out carefully to remove all the follicle cells and so avoid the presence of endogenous gonadotropin receptors.

Immunofluorescence Microscopy

Immunofluorescence microscopy was carried out on *X. laevis* oocytes injected with 30 or 10 ng of cRNA of *fshra*-FLAG and *lhcrba*-FLAG, respectively, or with water (control oocytes). Forty-eight hours after injection, oocytes were fixed in 4% paraformaldehyde for 4 h, subsequently dehydrated, and embedded in paraplast (Sigma). Sections (thickness, 7 μ m) were blocked with 5% goat serum and 0.1% bovine serum albumin (BSA) in PBST (137 mM NaCl, 2.7 mM KCl, 4.3 mM Na₂HPO₄, 1.4 mM KH₂PO₄, and 0.01% Tween; pH 7.5) and incubated overnight at 4°C with anti-FLAG antiserum (1:200; Rockland) in PBST with 1% goat serum and 0.1% BSA. Bound antibodies were detected with fluorescein isothiocyanate anti-rabbit secondary mouse antibodies (1:300; Sigma). Sections were mounted with Prolong Gold antifade reagent (Invitrogen), and photos were taken using a Leica SP2 confocal laser scanning microscope.

Functional Characterization of Senegalese Sole Gonadotropin Receptors

The ability of sole *Fshra* and *Lhcrba* to stimulate cAMP production in response to human chorionic gonadotropin (hCG; Sigma) and European sea bass (*Dicentrarchus labrax*) recombinant gonadotropins was tested in *X. laevis* oocytes expressing *fshra* or *lhcrba*. To produce the sea bass recombinant single-chain gonadotropins (sbFshsc and sbLhsc), the sequences coding for the alpha and beta subunits of Fsh and Lh were fused using overlapping PCR. As a linker between the subunits, the carboxy-terminal peptide from the hCG was used. These hybrid genes were cloned into the pcDNA3 expression vector (Invitrogen). Next, Chinese Hamster Ovary (CHO) cells were transfected and stable clones producing recombinant sbFshsc and sbLhsc derived. The production of recombinant gonadotropins was performed as described by Schatz et al. [56]. In brief, the CHO stable clones were grown in 75-cm² flasks at 37°C and 5% CO₂ in Dulbecco modified Eagle medium (DMEM)

supplemented with 100 U/ml of penicillin, 100 μ g/ml of streptomycin, and 5% fetal bovine serum (FBS). At 90% confluence, the growth medium was replaced by FBS-free DMEM, and the cells were further incubated for 7 days at 25°C. The conditioned medium was collected and concentrated with Centricon Plus-70 Ultracel PL 30 filter devices (Millipore). These preparations were quantified with in vitro bioassays consisting of HEK293 stable clones constitutively expressing the sea bass *fshra* or *lhcrba* [25] and the firefly luciferase gene under the control of a cAMP-responsive promoter. Sea bass receptor activation was measured by changes in luciferase activity and normalized to known concentration of homologous hormones that were used as standards.

For the experiments, groups of healthy defolliculated oocytes ($n = 10$) injected with water or expressing *fshra* or *lhcrba* were transferred to MBS supplemented with 100 μ M isobutylmethylxanthine (IBMX; Sigma) 48 h after injection. After 1 h, oocytes were incubated in triplicate with increasing concentrations of hCG (1–50 IU/ml) or sbFshsc and sbLhsc (100–1000 ng/ml) in MBS for 3 h. Control oocytes were exposed to water or to an equivalent volume of the cell culture medium used for sbFshsc and sbLhsc production. Intracellular cAMP was extracted by homogenizing oocytes, free of MBS, in 400 μ l of extraction buffer (99% ethanol and 1% HCl, supplemented with 100 μ M IBMX and 2.5 mM theophylline; Sigma). Samples were heated at 70°C for 10 min, followed by a 20-min centrifugation at 14 000 rpm at 4°C. The supernatant was recovered and the pellet resuspended in 100 μ l of the extraction buffer, centrifuged again for 20 min at 14 000 rpm at 4°C, and the supernatant mixed with the first extraction. Aliquots (50 μ l) of the ethanol extract from each replicate were dried at 65°C and the cAMP quantified using a cAMP competitive EIA kit (Cayman Chemical Company) following the manufacturer's instructions.

In Situ Hybridization

Samples of testes and ovaries were fixed in 4% paraformaldehyde for approximately 20 h at 4°C and subsequently dehydrated and embedded in Paraplast (Sigma). In situ hybridization on 7- μ m sections was carried out with digoxigenin-alkaline phosphatase (DIG-AP) incorporated riboprobes as previously described [42]. DIG-AP sense and antisense riboprobes were synthesized with T3 and T7 RNA polymerases using the DIG RNA labeling Kit (Roche). Probes were synthesized for sole *fshra* (nucleotides 2100–2439) and *lhcrba* (nucleotides 763–1555) as well as for the Senegalese sole steroidogenic acute regulatory protein-related protein (*star*) as a marker for Leydig cells. The *star* riboprobes were synthesized from clone pgsP0030J11 (GenBank accession no. FF291770 [57]) bearing the full-length cDNA. The DIG-labeled RNA probes were detected as described previously [42]. The resulting dark blue to purple color indicated localization of the transcripts. In some cases, sections were counterstained with Nuclear fast red. All sections were examined and photographed with a Leica DMLB light microscope.

Real-Time Quantitative PCR

Total RNA from adult tissues, including ovary and testis, as well as from dissected ovarian follicles was isolated as previously described. First-strand cDNA was synthesized from 0.5 μ g of total RNA by using 0.5 μ g of oligo(dT)₁₇, 1 mM dNTPs, 40 IU of RNase inhibitor, and 10 IU of AMV RT enzyme (Roche) for 1.5 h at 42°C. One negative control (without RT) was included in each experiment. Real-time quantitative PCR (qPCR) amplifications were performed in a final volume of 20 μ l with 10 μ l of SYBR Green qPCR master mix (Applied Biosystems), 1 μ l of diluted (1:10) cDNA, and 0.5 μ M each primer (Supplemental Table S1). The sequences were amplified in duplicate for each sample on 384-well plates using the ABI PRISM 7900HT sequence detection system (Applied Biosystems). The amplification protocol was an initial denaturation and activation step at 50°C for 2 min and 95°C for 10 min, followed by 40 cycles of 95°C for 15 sec and 63°C for 1 min. After the amplification phase, a temperature-determining dissociation step was carried out at 95°C for 15 sec, 60°C for 15 sec, and 95°C for 15 sec. For normalization of cDNA loading, all samples were run in parallel using Senegalese sole glyceraldehyde-3-phosphate dehydrogenase 1 (*gapdh1*) [58] or 18S ribosomal protein (*18s*) as reference genes for testis and for ovary and ovarian follicles, respectively, because their expression between experimental samples did not show significant differences (data not shown). To estimate efficiencies, a standard curve was generated for each primer pair from 10-fold serial dilutions (from 100 to 0.01 ng) of a pool of first-stranded cDNA template from all samples. Standard curves represented the cycle threshold value as a function of the logarithm of the number of copies generated, defined arbitrarily as one copy for the most diluted standard. All calibration curves exhibited correlation coefficients higher than 0.98, and the corresponding qPCR efficiencies were greater than 99%.

Statistical Analysis

Data are presented as the mean \pm SEM. Data regarding oocyte cAMP production and the relative expression of *fshra* and *lhcrba* during gametogenesis were statistically analyzed by one-way ANOVA. Values were log-transformed when the variances were not homogeneous. The significance level was set at 0.05.

RESULTS

Molecular Characterization of Senegalese Sole *Fshr* and *Lhcgr*

By using degenerate primers and 5' and 3' end RACE, the full coding sequences of *S. senegalensis fshra* and *lhcrba* were isolated. The cloned *fshra* cDNA covers a total of 2819 nucleotides with an open-reading frame from nucleotides 67 to 2157, encoding a polypeptide of 696 amino acids (Supplemental Fig. S1). The *lhcrba* cDNA is 2365 nucleotides with a predicted open-reading frame from nucleotides 38 to 2149, giving a protein of 703 amino acids (Supplemental Fig. S2). Both *Fshra* and *Lhcgrba* retain a signal peptide of 20 and 24 amino acids, respectively, and share 40% identity.

The Senegalese sole gonadotropin receptors have conserved overall structures that are consistent with vertebrate GpHRs [29]: a signal peptide; an N-terminal extracellular domain, which harbors the ligand-binding domain (LBD) formed by an extended concave β -sheet barrel that recognizes the cognate hormone; a short linker domain; a well-conserved 7TMD; and a short intracellular C-terminal segment (Supplemental Figs. S3 and S4). As in other members of the GpHR family, the sole *Fshra* and *Lhcgrba* LBDs share low sequence identity (30%). The LBDs are composed of 11 and 10 LRRs in *Fshra* and *Lhcgrba*, respectively, containing the consensus sequence **XXLXLXX**, where X can be any amino acid and L is leucine, valine, isoleucine, or other hydrophobic amino acid [59].

Alignment of the deduced amino acid sequences against orthologs in Teleostei and Tetrapoda revealed that as in our earlier study with the European sea bass [25], the additional LRR in sole *Fshra* comprises a 25 amino acid segment between Ser¹¹¹ and Leu¹³⁵. We found that this segment is encoded within the *Fshra* of all Acanthomorpha (spiny-ray-finned fishes) but is not present in the *Fshra* of lower teleosts (Protacanthopterygii, Ostariophysii, and Elopomorpha), tetrapods, or vertebrate *Lhcgrs*. To determine whether the additional 25-amino-acid segment represents a splice variant, we aligned the sole *fshra* cDNA against the exon structures of *fshr* from available teleost genomes. These data showed an additional exon within the acanthomorph species that is lacking in zebrafish (Supplemental Fig. S5). Senegalese sole *fshra* closely resembles the gene structures in stickleback (exons 2–12), green-spotted pufferfish (exons 1–11) and medaka (exons 3–14), and likely is encoded by 12–14 exons. Interestingly, however, medaka exons 3 and 4 represent duplicated nucleotide regions. Exon 4 in medaka maps to exon 2 in green-spotted pufferfish and the C-terminal fraction of exon 2 in stickleback, and because this region is absent in the genomic structures of lower Teleostei and Tetrapoda, we conclude that the additional 25-amino-acid segment in Senegalese sole *Fshra* is not a splice variant but, rather, represents a gene variant found only within the Acanthomorpha.

Three-dimensional modeling of sole *Fshra* against the crystallographically resolved structure of human FSHR showed that the extra 25-amino-acid segment putatively folds as an additional β -sheet barrel (β 3b) between β 3 and β 4 (Fig. 1). This locus within the concave surface of the LBD may serve to increase the receptor area for ligand interaction and is

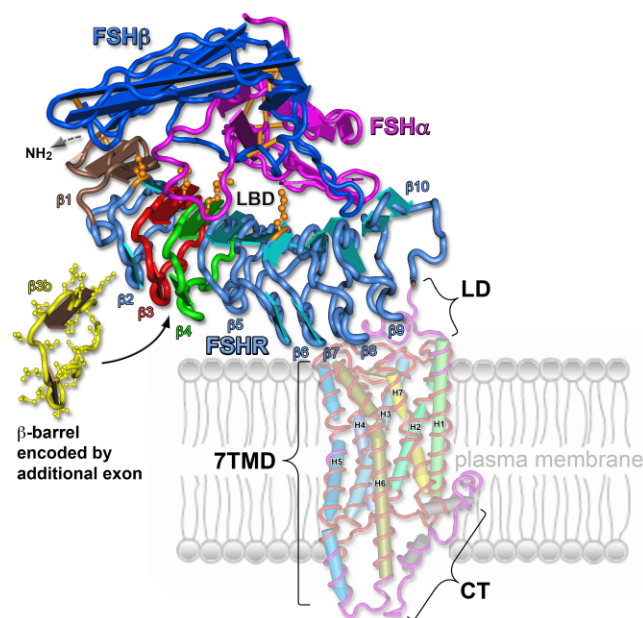


FIG. 1. Three-dimensional render of the Senegalese sole *Fshra* LBD mapped to the crystallographically resolved structures of human FSHR and squid rhodopsin. The first β -sheet of each leucine-rich repeat in the LBD is numbered 1–10. The α (magenta) and β (blue) chains of human FSH are shown to highlight the β -sheet barrels (β 3 red and β 4 green) at the interacting domain. Side chains of residues implicated with binding specificity in the human molecule are shown as orange ball and stick renders. The acanthomorph-specific β 3b barrel (yellow) localizes between β 3 and β 4. The FSHR render terminates at the linker domain (LD) extending down to the rhodopsin G-coupled membrane-anchoring complex (7TMD). The transmembrane helices are numbered 1–7 toward the C-terminal domain (CT).

specifically located within the interaction domain [49]. The putative amino acids (nonsuperscript) that interact with sole *Cga* and *Fshb* are R^VI^LG, D^LI^SG, and E^TT^IN for β 3, β 3b, and β 4 barrels, respectively (Supplemental Fig. S3). Matching sequences for human FSHR are K^LE^IQ and E^RI^EK for β 3 and β 4 barrels, respectively.

The more conserved region between sole *Fshra* and *Lhcgrba* (61% identity), and also between different species of teleosts, is the 7TMD membrane-anchoring complex, which shows highly conserved extra- and intracellular loops. A molecular wrap of this domain to the structure mask of squid rhodopsin [60] reveals that the sole *Fshra*-7TMD conforms to the tertiary structure of this class of G protein-coupled receptors (Fig. 1). The extracellular loops 1 and 2 of sole *Fshra* and *Lhcgrba* carry conserved cysteine residues (Supplemental Figs. S3 and S4) that tether the loops and may interact together to form a disulfide bridge compulsory for membrane anchoring [61]. However, the DRY motif at the C-terminus of α -helix 3, which is considered important for receptor activation [61], is alternatively conserved as a consensus ERW in the sole and other vertebrate GpHRs (Supplemental Figs. S3 and S4). Compared to the 7TMD, the intracellular C-terminus domain is highly divergent between species and between receptors (14% identity between sole *Fshra* and *Lhcgrba*). The sole *Fshra* C-terminus showed four conserved putative protein kinase C phosphorylation sites (S/T-X-R/K), whereas *Lhcgrba* had none. Conversely, *Lhcgrba* retains the conserved membrane-anchoring Cys⁶⁵⁷-Cys⁶⁵⁸ doublet found in other vertebrate *Lhcgrs*, whereas sole *Fshra* and vertebrate *Fshrs* and *Tshrs* do not. With respect to other teleost orthologs, however, we found that sole *Fshra* shares greater homology to acanthomorph *Fshrs* (66% \pm

5%) compared to *Fshrs* in non-Acanthomorph species (52% \pm 2%) (Supplemental Table S2). By contrast, sole *Lhcgrba* has higher identity (68% \pm 6% vs. 45% \pm 1%) to selected teleost *Lhcgrs*, regardless of phylogenetic position.

Phylogenetic Analyses

Phylogenetic characterization of the codons and deduced proteins confirmed the orthologous relationships of the Senegalese sole *Fshra* and *Lhcgrba* paralogs within the Gnathostomata (Fig. 2). Tree topologies were highly robust and resolved teleost *gphr* codons and GpHR proteins as sister branches to tetrapod *FSHR*, *LHCGR*, and *TSHRs*, respectively. Despite retaining the extra β 3b barrel within the LBD, sole *fshra* and *Fshra* clustered as a typical Acanthomorph *Fshr* in full congruence with its pleuronectiform position. Deletion of the β 3b barrel did not affect the tree topology (data not shown). Whereas all teleost *fshr* isoforms clustered in accordance with their phylogenetic rank, *lhcgr* isoforms differentially clustered as two subbranches within the teleost crown clade. Even the *lhcgr* transcripts and *Lhcgr* proteins of closely related species within Pleuronectiformes (tongue sole and Atlantic halibut) did not cluster with sole *lhcgrba*. We therefore hypothesized that Teleostei retain two *lhcgr* isoforms resulting from the whole genome duplication (R3 WGD) that occurred at the root of the crown clade [51, 62, 63]. However, screening of genomic databases via BLAST revealed only single-copy variants, of which only zebrafish *lhcgr* clustered on the same subbranch as sole *lhcgrba*, whereas Acanthomorph genomic *lhcgr* transcripts and *Lhcgr* proteins clustered on the sister branch.

Synteny Analysis of Tetrapod and Teleost *FSHR* and *LHCGR*

To further elucidate the basis of the *lhcgr* branching topology, we investigated the syntenic relationships between teleost and tetrapod GpHRs (Fig. 3 and Supplemental Fig. S6). This analysis revealed the close tandem arrangement of *LHCGR-FSHR* in the majority of tetrapod genomes, with slight rearrangement in humans, wherein *LHCGR* and *FSHR* are separated by a fragment of the *STONED* (*STON1-GTF2AIL*) gene that flanks the other tetrapod GpHRs. In Teleostei, *lhcgr* and *fshr* are also present as single-copy genes, but on separate chromosomes. Whereas these findings did not reveal the expected dual-gene synteny between Teleostei and Tetrapoda, we were able to identify the two GpHR-retaining paralogs that are syntenic to the tetrapod orthologs. By tracing closely linked members of three other gene families, the potassium channels (*KCNK12* and *KCNK13*), the forkhead box proteins (*FOXN2* and *FOXN3*), and the neurexins (*NRXN1* and *NRXN3*), it was possible to validate the common heritage of the three gnathostome GpHRs. In fact, the molecular phylogenies of the teleost and tetrapod GpHRs precisely reflect their physical maps within the respective genomes. Teleostei have two WGD products of *tshr* but appear to have preferentially retained *tshra* genes with conserved syntenies to tetrapod *TSHR* orthologs. Conversely, Teleostei have only one of the WGD *fshr* products (*fshra*) that has maintained its syntenic relationship to tetrapod orthologs, regardless of phylogenetic

rank. The heritage of the teleost *lhcgr* genes, however, appears to be more complex. Acanthomorph *lhcgr* orthologs show conserved linkage maps and have higher synteny to tetrapod orthologs. By contrast, the ostariphysan zebrafish *lhcgr* has reduced synteny to both the Acanthomorph and tetrapod orthologs, yet it is the ortholog that clusters on the same subbranch as sole *lhcgrba* independent of the method of phylogenetic inference. We therefore hypothesized that the secondary clustering or teleost *lhcgrs* might reflect the alternate WGD product.

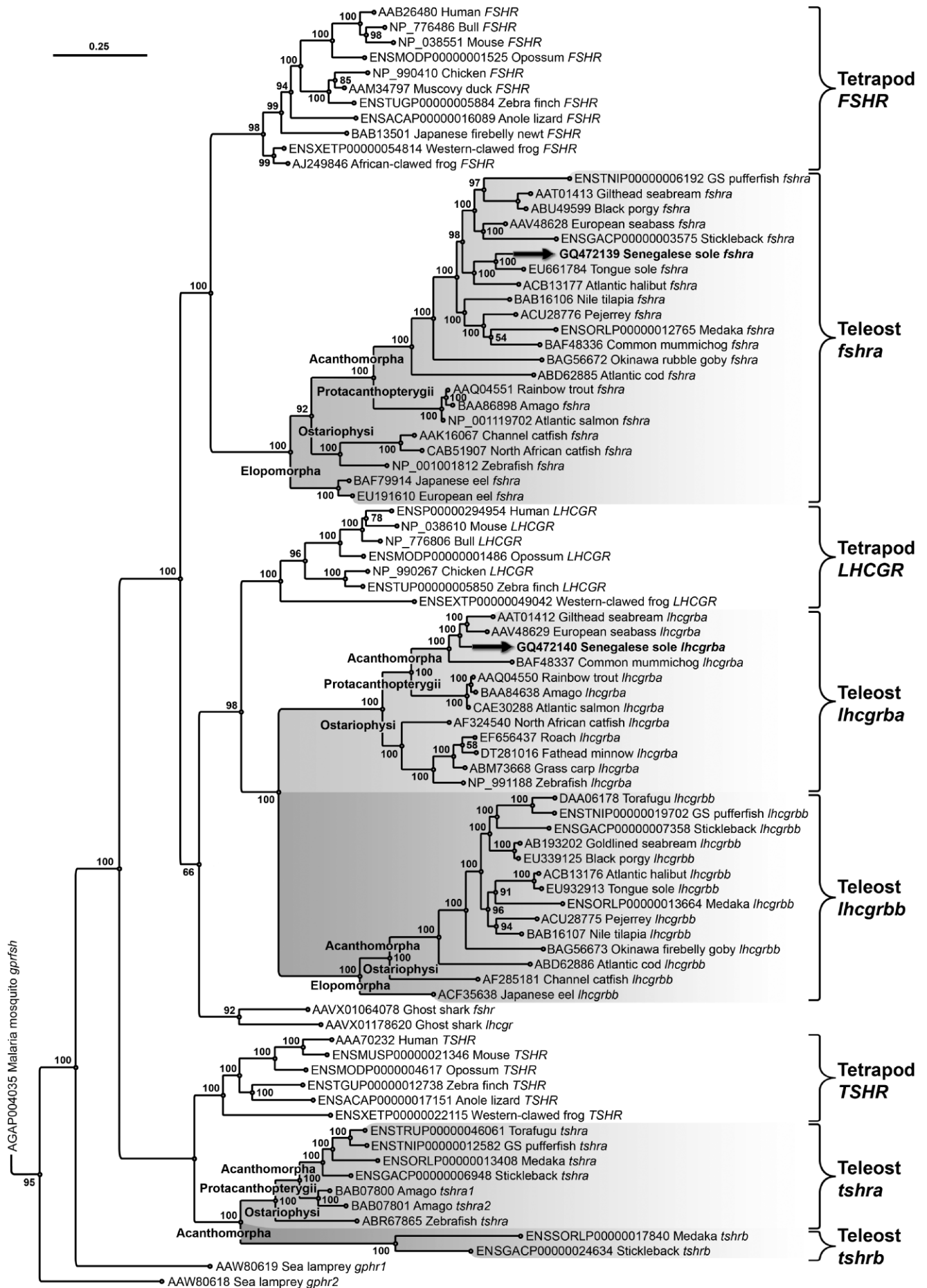
To investigate this possibility, we conducted a molecular phylogenetic analysis of the flanking *NRXN* genes. The *NRXN* genes are members of a broader family of proteins that contain laminin G domains, which were originally identified as synaptic transmembrane receptors that recognize arachnid venom [64]. In the present context, these genes have the advantage of offering more complete genomic complements for classifying the history of the *GpHR* loci. ML and Bayesian analyses of 65 vertebrate *NRXN* codons and deduced *NRXN* amino acid sequences generated resolved tree topologies that are consistent with their mapped loci (Supplemental Fig. S7). Tetrapod *NRXNs* robustly separate as three isoforms (*NRXN1*, *NRXN2*, and *NRXN3*), whereas teleost isoforms cluster as orthologous branches (*nrxn1a*, *nrxn1b*, *nrxn2a*, *nrxn2b*, *nrxn3a*, and *nrxn3b*). We noted, however, that most vertebrates have tandem duplicates of the *NRXN* genes. By integrating the phylogenetic data with the physical loci, we were able to classify the teleost *nrxns* as *aa*, *ab*, *ba*, or *bb*, where the prefix *a* or *b* represents the R3 WGD product and the postscript *a* or *b* represents a tandem duplicate.

The analysis of *NRXN* genes helped to classify the teleost paralogs that harbor the single *fshr* and *lhcgr* genes as well as the duplicated *tshr* genes. The conserved paralogs containing teleost *fshr* isoforms all mapped with *nrxn1a*, and we therefore classified these GpHRs as *fshra*. Conversely, only the Acanthomorph *lhcgr*-retaining paralogs map with *nrxn1b* or *nrxn1bb* genes, whereas the zebrafish paralogon (chromosome 12), which displays reduced synteny, maps with *nrxn1ba*. Comparison of the physical synteny with the alignment synteny (Supplemental Fig. S6), however, revealed that most of the flanking orthologs on the zebrafish *b* paralogon are present but have been rearranged, which is an observation we have noted for other gene systems [65]. Considering the broad, family-level phylogenetic analysis of the single teleost *lhcgr* sequences and the absence of duplicates in the genomes, the available evidence suggests that *lhcgr* has not duplicated but could represent the result of gene conversion. Based upon the phylogenetic and syntenic data, we classified the teleost *lhcgr* genes as *lhcgrba* or *lhcgrbb*, wherein the Senegalese sole expresses *lhcgrba*.

Functional Analysis of Senegalese Sole *Fshra* and *Lhcgrba* in *X. laevis* Oocytes

To investigate if sole *fshra* and *lhcgrba* encoded functional proteins, the corresponding cRNAs were expressed in *X. laevis* oocytes, which are often used as a heterologous system for the functional expression of membrane proteins including gonad-

FIG. 2. Maximum likelihood phylogeny of aligned vertebrate glycoprotein hormone receptors. The tree is rooted with the malaria mosquito (*Anopheles gambiae*) *gprish* ortholog. Bayesian posterior probabilities for phylogenetic analyses of the codon and amino acid alignments are shown at each node, respectively. Black arrows highlight the Senegalese sole *fshra* and *lhcgrba* receptors, respectively. The scale bar calibrates the branch lengths, which indicate the number of nucleotide substitutions per site. Ensembl and GenBank accession numbers are annotated with the taxa.



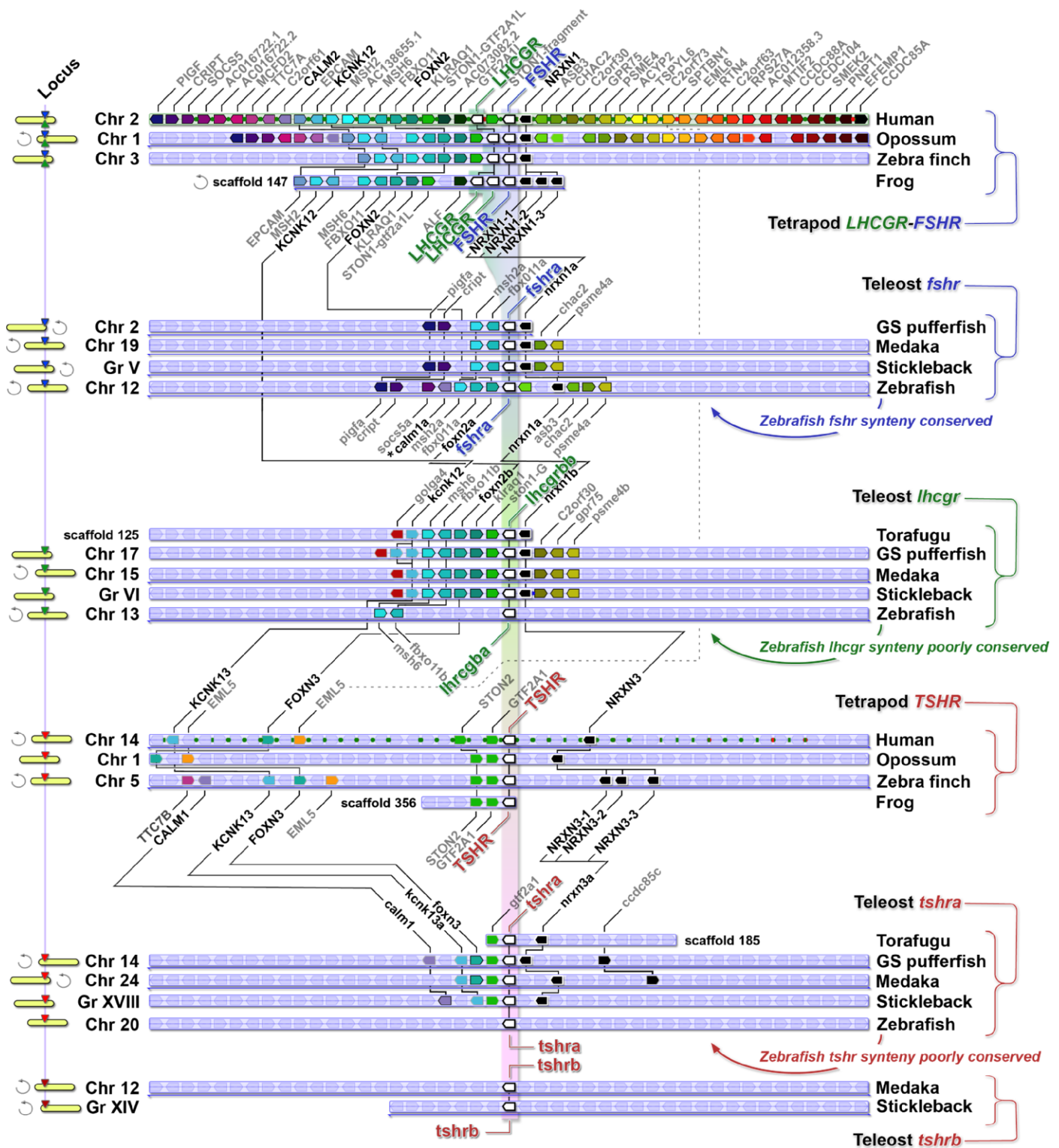


FIG. 3. Physical synteny of orthologons harboring the vertebrate glycoprotein hormone receptor loci for *LHCGR*, *FSHR*, and *TSHR*. Receptor genes are shown in white and neurexin genes in black, with the coding direction indicated by the pointed end. Empty pale blue symbols indicate nonsyntenic genes. Circular arrows beside chromosomal loci (left) indicate that the orthologon is flipped. Genes with highly conserved linkage maps are traced and annotated in bold black. *See Supplemental Figure S6 for an explanation of the zebrafish *calm1a* annotation on chromosome 12.

otropin receptors [66, 67]. In these experiments, ligand-induced cAMP production in oocytes was determined using hCG and sea bass single-chain recombinant gonadotropins (Fig. 4). Oocytes injected with sole *fshra*-FLAG and *lhcrba*-FLAG specifically displayed the target proteins in the plasma

membrane (Fig. 4, B and C), whereas water-injected oocytes showed no immunofluorescence (Fig. 4A). Incubation of sole *Fshra*- and *Lhcrba*-expressing oocytes with hCG induced a dose-dependent stimulation of intracellular levels of cAMP compared to controls injected with water (Fig. 4D, left). The

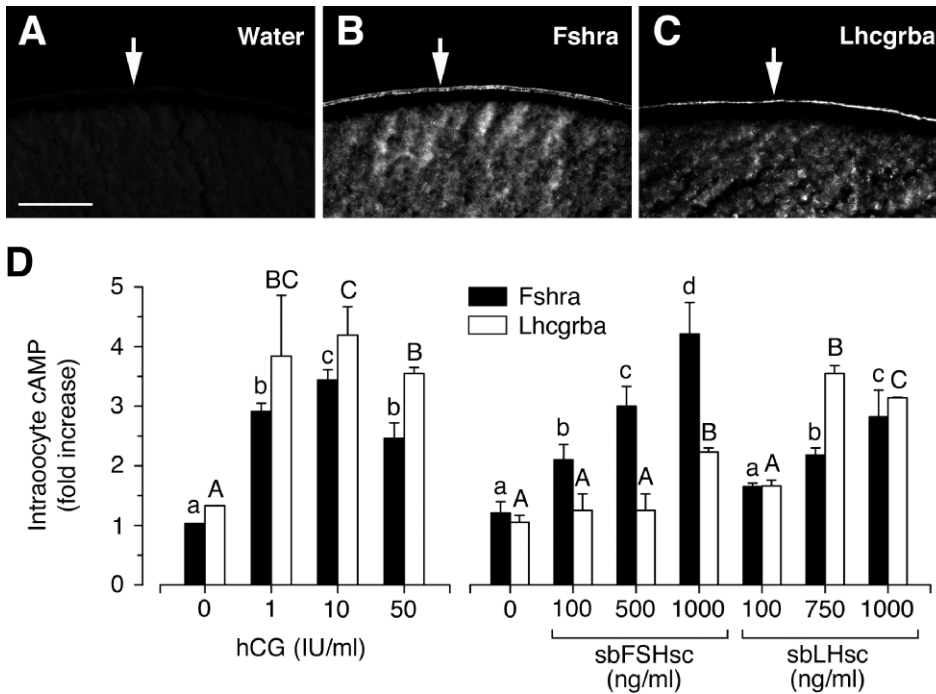


FIG. 4. Functional characterization of Senegalese sole *Fshra* and *Lhcgrba* in *Xenopus laevis* oocytes. **A–C** Immunofluorescence microscopy of oocytes injected with water (**A**), 30 ng of *Fshra*-FLAG cRNA (**B**), or 10 ng of *Lhcgrba*-FLAG cRNA (**C**) using the anti-FLAG antibody. The arrows point to the localization of expressed proteins at the oocyte plasma membrane. Bar = 50 μ m. **D**) Production of cAMP indicated as fold-increase with respect to water-injected oocytes of *Fshra*- and *Lhcgrba*-expressing oocytes exposed to increasing concentrations of hCG or European sea bass single-chain recombinant gonadotropins (sbFshsc and sbLhsc). Data are presented as the mean \pm SEM of a representative experiment in which each treatment was in triplicate. Data with different superscripts within oocyte groups expressing the same receptor are significantly different (ANOVA, $P < 0.05$).

highest hCG dose (50 IU/ml) resulted in reduced cAMP production when compared to that obtained with 10 IU/ml of hCG.

In subsequent experiments, oocytes were incubated with different doses of sbFshsc and sbLhsc (100–1000 ng/ml). The results showed that sole *Fshra* responded in a dose-dependent manner to sbFshsc, whereas the *Lhcgrba* did not respond to this hormone up to concentrations of 500 ng/ml (Fig. 4D, right). At the highest incubation dose (1000 ng/ml), however, a significant induction of cAMP (twofold increase) was observed for *Lhcgrba*-expressing oocytes. In contrast to these experiments, increasing concentrations of sbLhsc caused dose-dependent activation of both *Fshra* and *Lhcgrba*, although the cAMP levels were attenuated at 1000 ng/ml of sbLhsc (Fig. 4D, right). Based upon these data, we concluded that the gonadotropin receptors isolated from Senegalese sole were functionally active.

Analysis of Senegalese Sole *fshra* and *lhcgrba* mRNA Expression

The tissue expression of sole *fshra* and *lhcgrba* was examined in sexually mature fish by qPCR using gene-specific primers. Both receptors seemed to be highly expressed in the gonads, but the relative levels of mRNA expression appeared to be higher in the testis than in the ovary (Fig. 5). Interestingly, whereas the expression of *lhcgrba* was gonad specific, low levels of *fshra* were noted in the pituitary gland, muscle, and gills.

Samples of ovaries and testes were further selected to determine the cell types expressing *fshra* and *lhcgrba* by in situ hybridization. Experiments carried out on ovarian sections, however, were not successful despite repeated efforts using different cRNA probes and ovaries at different developmental stages (data not shown). This may suggest very low expression levels of native *fshra* and *lhcgrba* in the sole ovary. In testes, *fshra* was localized specifically in Sertoli cells, whereas no positive signal was detected in interstitial cells or in germ cells at any developmental stage (Fig. 6, A and B). Expression of *lhcgrba* was observed in Leydig cells (Fig. 6, D and E), which

were also labeled with antisense probes for *star* (Fig. 6, G and H), as well as in Spd (Fig. 6, D and E). No *lhcgrba* signal was detected in Sertoli cells. In all the experiments, sense probes gave no signal (Fig. 6, C, F, and I).

Expression of Sole *fshra* and *lhcgrba* in the Ovary During Oocyte Growth and Maturation

To identify the putative regulatory roles the gonadotropin receptors play during ovarian development in Senegalese sole, we determined the expression profiles of *fshra* and *lhcgrba* in the ovary during sexual maturation by qPCR (Fig. 7). The

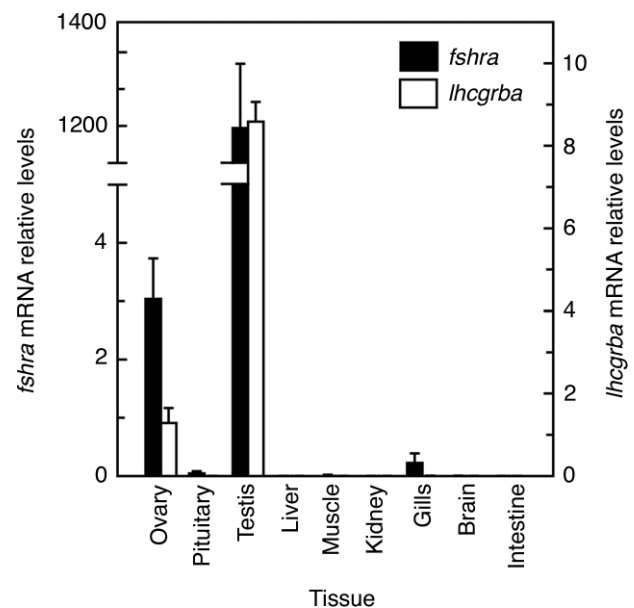
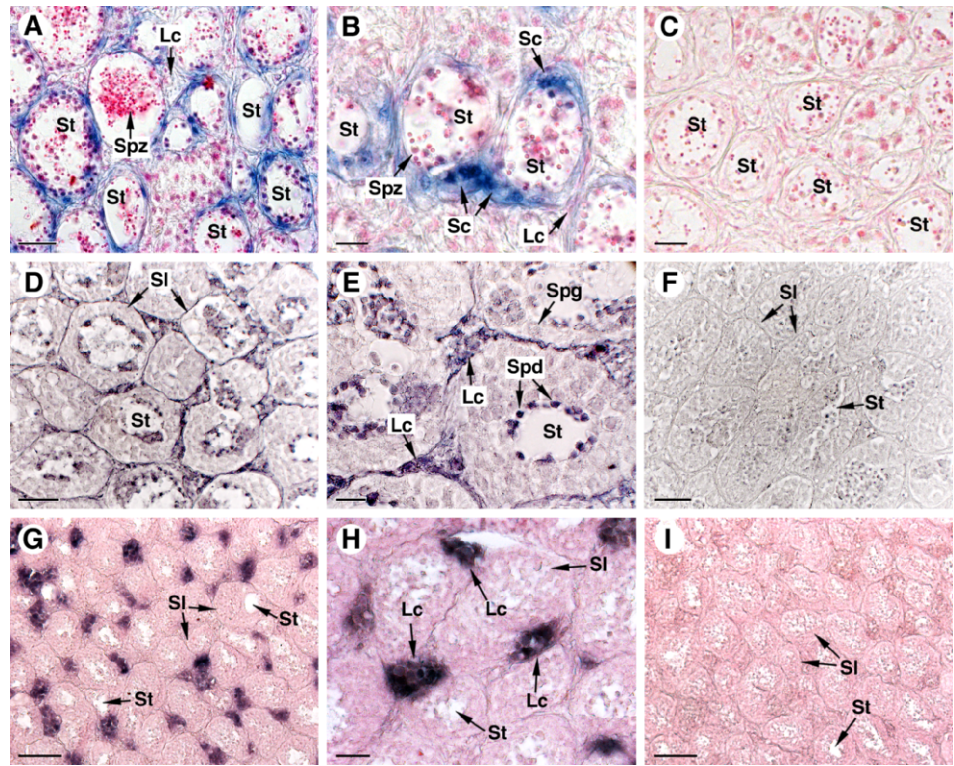


FIG. 5. Tissue distribution of Senegalese sole *fshra* and *lhcgrba* mRNA expression. Total RNA from each tissues was subjected to qPCR using *18s* as reference gene. Data are presented as the mean \pm SEM ($n = 3$ different cDNAs from three different animals).

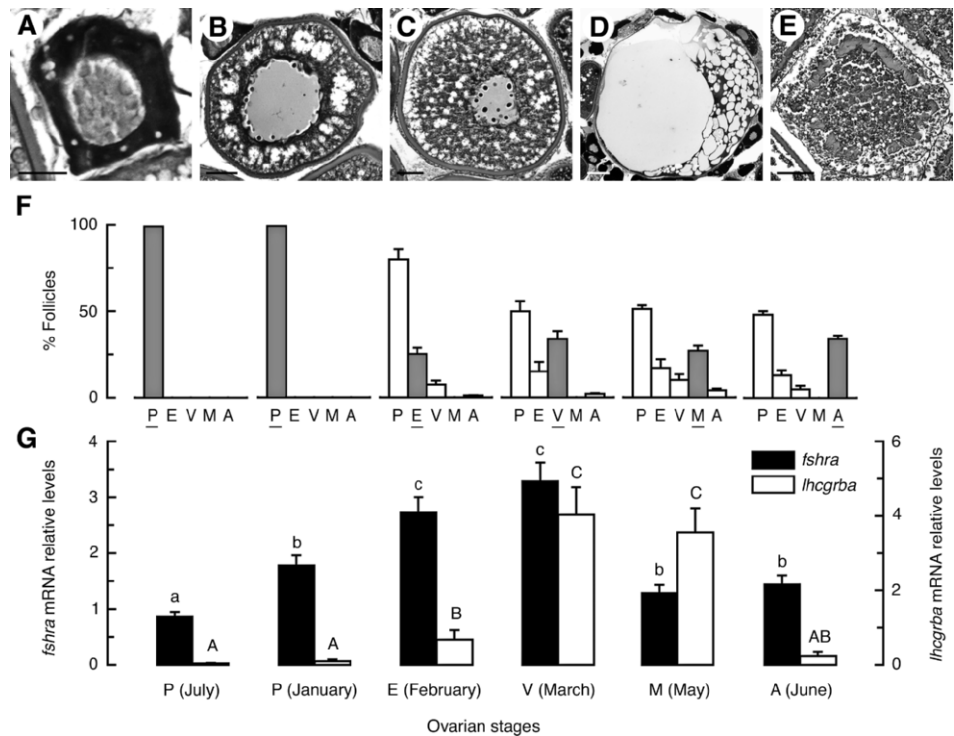
FIG. 6. Localization of Senegalese sole *fshra*, *lhcrba*, and *star* in histological sections from the testis by in situ hybridization using DIG-labeled antisense riboprobe. **A** and **B**) Expression of *fshra* in Sertoli cells. **D** and **E**) Expression of *lhcrba* in Leydig cells and Spd. **G** and **H**) Expression of *star* in Leydig cells. Sections shown in **A**–**C** and **G**–**I** were counterstained with Nuclear fast red. Lc, Leydig cells; Sc, Sertoli cells; Sl, seminiferous lobule; Spd, spermatid; Spg, spermatogonia; Spz, spermatozoa; St, seminiferous tubule. Bar = 10 μ m (**B** and **E**), 20 μ m (**A**, **C**, and **H**), 40 μ m (**D** and **F**), 60 μ m (**G** and **I**).



experiment started with ovarian samples collected from sexually immature fish in July, and samples of ovaries were subsequently collected at the onset of the reproductive cycle (January) through vitellogenesis (February and March), GnRH α -induced maturation (May), and ovarian atresia (June). Because Senegalese sole exhibits group-synchronous ovarian development [68], a sample of ovarian tissue from each female collected was fixed for histological determination of the specific stage of ovarian development. As shown in Figure

7F, ovaries collected in July and January retained exclusively previtellogenic follicles at the primary growth stage (Fig. 7A), whereas the appearance of early vitellogenic (Fig. 7B), vitellogenic (Fig. 7C), mature (Fig. 7D), and atretic (Fig. 7E) ovarian follicles (in ovaries collected in February, March, May, and June, respectively) established the specific stage of ovarian development. Atretic ovaries contained 20–30% irregularly shaped vitellogenic follicles in which oocytes had shrunk and the zona radiata was folded.

FIG. 7. Expression of Senegalese sole *fshra* and *lhcrba* in the ovary during ovarian growth, maturation, and atresia. **A**–**E**) Photomicrographs of Senegalese sole ovarian follicles at previtellogenesis or primary oocyte growth (**A**), early vitellogenesis (**B**), vitellogenesis (**C**), maturation (**D**), and atresia (**E**). Bar = 50 μ m (**A**–**C**), 100 μ m (**D** and **E**). **F**) Percentage of ovarian follicles at previtellogenesis (P), early vitellogenesis (E), vitellogenesis (V), maturation (M), and atresia (A) in the ovary during July, January, February, March, May, and June. **G**) Sole *fshra* and *lhcrba* expression levels in ovaries at different developmental stage as determined by qPCR. The mRNA levels were normalized to 18s and are presented as the mean \pm SEM (n = 3–5 females). Within each receptor, values with different superscript are significantly different (AN-OVA, $P < 0.05$).



The qPCR experiments revealed that in the previtellogenic ovary, only *fshra* was expressed, whereas *lhcrba* was barely detectable (Fig. 7G). The average level of *fshra* mRNA in the ovary gradually increased as vitellogenesis advanced, then dropped at the maturation and atretic stages. In contrast, the level of *lhcrba* mRNA was generally low during previtellogenesis and early vitellogenesis but strongly increased at the vitellogenic stage in March. The *lhcrba* levels remained high at the maturation stage and, during atresia, decreased to a level comparable to that found in previtellogenic follicles.

To further confirm the stage-dependence of *fshra* and *lhcrba* expression in the sole ovary, we carried out another experiment to examine the expression of the two receptors in manually isolated ovarian follicles at different developmental stage collected from sexually mature females (Fig. 8). The results demonstrated a similar but clearer stage-dependent expression of *fshra* and *lhcrba* compared to that observed at the level of the ovary. Previtellogenic and early vitellogenic ovarian follicles (<0.250 mm) (Fig. 8A) clearly expressed *fshra*, whereas *lhcrba* had extremely low expression (Fig. 8E). With the advancement of vitellogenesis, expression of *fshra* increased in vitellogenic follicles (Fig. 8B), but levels of *lhcrba* mRNA were also markedly accumulated. In mature (Fig. 8C) and atretic (Fig. 8D) follicles, both *fshra* and *lhcrba* mRNA levels dropped drastically, the reduction being more dramatic for *lhcrba*. These observations are consistent with *fshra* being associated with follicular growth and development, whereas *lhcrba* seems to be accumulated specifically during late vitellogenesis.

Expression of Sole *fshra* and *lhcrba* in Testis During Spermatogenesis

The testis of Senegalese sole is asynchronous; therefore, it carries all stages of germ cell development throughout the reproductive cycle [69]. However, during winter (January and February), when the temperature is low ($\leq 10^{\circ}\text{C}$), plasma levels of testosterone and 11-ketotestosterone usually rise, and meiosis is initiated, resulting in an increased prevalence of Spc [42, 69–71]. During spring, plasma androgen levels tend to decrease, the number of Spd in the testis progressively diminishes as successive batches transform into Spz, and spermiation slightly increases. Therefore, to investigate the differential expression of *fshra* and *lhcrba* in the Senegalese sole testes during spermatogenesis, animals under a controlled temperature regime were collected in August, February, and May (Fig. 9). Histological examination of the testes of these animals showed that the percentage of SgB and Spc significantly increased during February, whereas in May, the relative fraction of Spd decreased and the number of Spz per seminiferous tubule increased (Fig. 9, A and B). A substantial increase in testicular *fshra* and *lhcrba* mRNA levels was observed in February, at the time when spermatogenesis was stimulated (Fig. 9C). In May, when spermiation increased, the *fshra* mRNA levels dropped to a level comparable to that found in August, whereas those of *lhcrba* diminished but remained significantly higher than in August (Fig. 9C).

DISCUSSION

In the present study, we cloned the full-length cDNAs for both *fshra* and *lhcrba* in the Senegalese sole, which represents the second Pleuronectiform species in addition to Atlantic halibut [26, 27], with both receptors cloned and characterized.

Phylogenetic analysis of the receptors revealed a robust topology of the *fshra* transcripts that is congruent with species

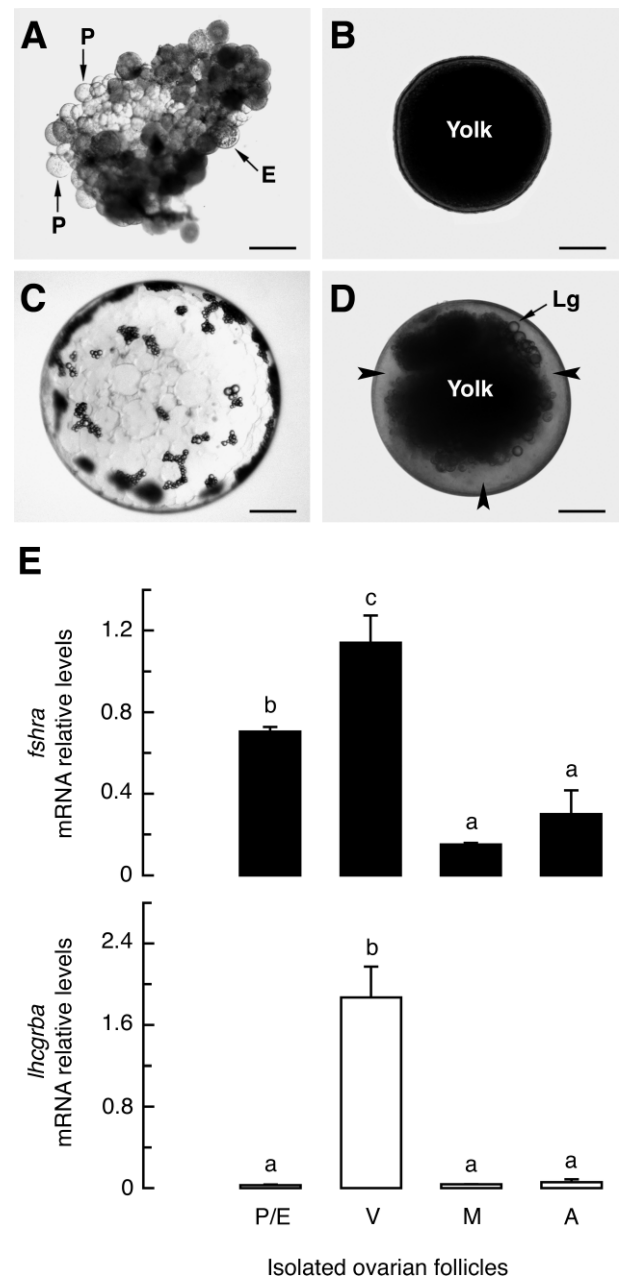
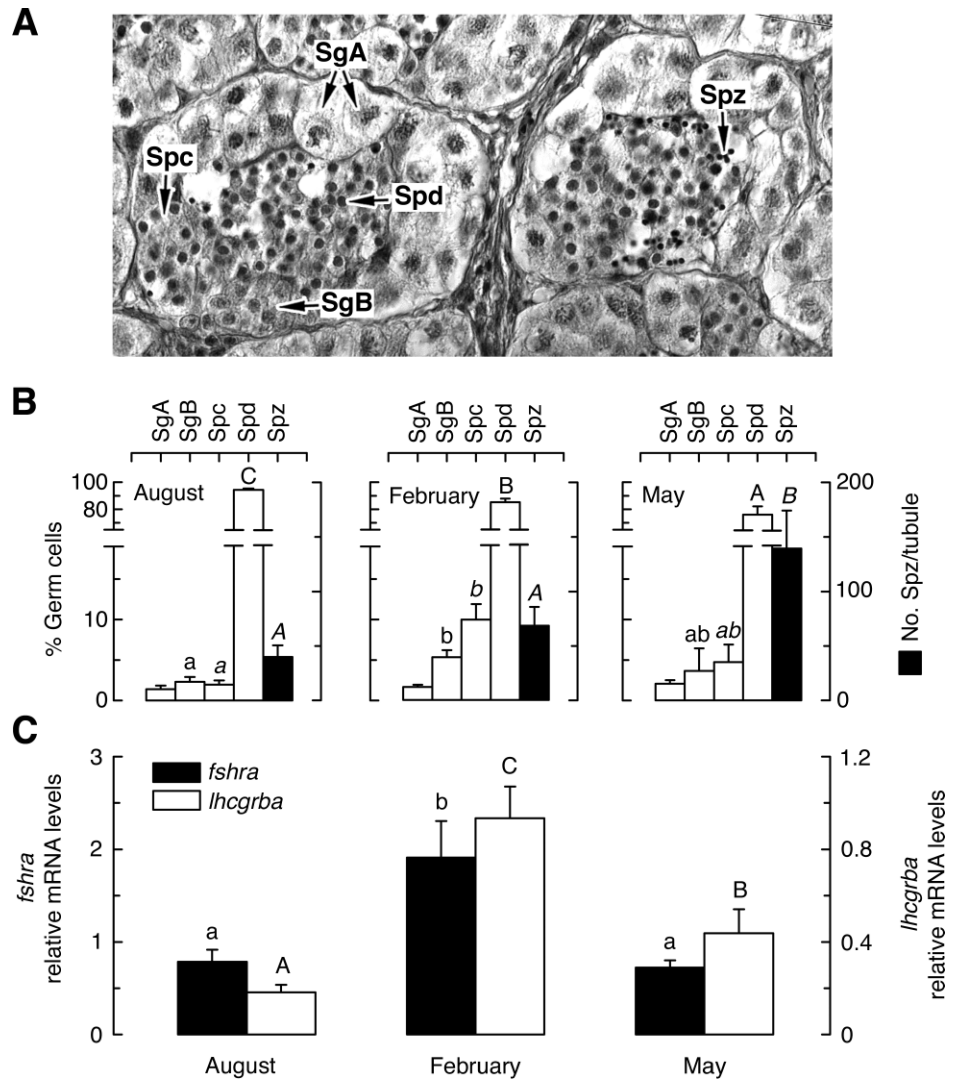


FIG. 8. Stage-dependent expression of sole *fshra* and *lhcrba* in ovarian follicles. **A–D**) Follicles at previtellogenesis (P) and early vitellogenesis (E; **A**), vitellogenesis (V; **B**), maturation (M; **C**), and atresia (A; **D**) were isolated and the total RNA used for qPCR. In **D**, the contraction of yolk during atresia (arrowheads) leaves lipid globules (Lg) visible. Bar = 50 μm (**A**) and 200 μm (**B–D**). **E**) *fshra* and *lhcrba* expression levels in each follicle stage were normalized to *18s*. Data are presented as the mean \pm SEM ($n = 3$ different batches of follicles from three females). Values with different superscript in each panel are significantly different (ANOVA, $P < 0.05$).

diversification. We therefore conclude that the single *fshra* isoforms in Teleostei are descended from a common ancestral gene. However, we found an unexpected complexity of the *lhcrba* transcripts that was translated to the proteins. Within the teleost crown clade, *lhcrba* transcripts cluster across all phyla as two sister branches, both of which are orthologous to tetrapod *LHCGR*. An earlier report documenting the cloning and expression of *fshra* and *lhcrbb* in Atlantic halibut [26] proposed that the observed sequence variation of the transcripts

FIG. 9. Expression of *fshra* and *lhcrba* in the sole testis during spermatogenesis. **A**) Photomicrograph of a histological section of Senegalese sole testis stained with hematoxylin and eosin where spermatogonia A (SgA), spermatogonia B (SgB), spermatocytes (Spc), spermatids (Spd), and spermatozoa (Spz) can be observed. Bar = 20 μ m. **B**) Percentage of germ cells (mean \pm SEM, n = 10 males) in the testis during summer (August), winter (February), and spring (May). For each germ cell type, values with different superscripts are significantly different (ANOVA, $P < 0.05$). **C**) *fshra* and *lhcrba* expression levels in testis during August, February, and May. The mRNA levels were normalized to *gapdh1* and are presented as the mean \pm SEM (n = 10 males). For each receptor, values with different superscript are significantly different (ANOVA, $P < 0.05$).



and deduced proteins of Atlantic halibut *fshra* and a second zebrafish *lhcrb* were the result of the teleost-specific WGD. However, the second zebrafish *lhcrb* (GenBank accession number: LOC572416) was located on an unclassified chromosome and has been removed as a result of standard genome annotation processing. Consequently, only single *lhcrb*-type genes are currently located within teleost genomes, and to our knowledge, duplicate *lhcrb* transcripts have not been cloned from any species. Considering that chordate GpHRs evolved from a common ancestor that also gave rise to type A *LGR* orthologs in invertebrates [3, 72], and that Agnatha already possessed two GpHRs that correlate to the *LHCGR/FSHR* and *TSHR* subfamilies [73, 74], some loss of GpHR genes must have occurred within the vertebrate lineage. As proposed for the cognate hormones, LH and FSH [4, 75], the appearance of *LHCGR* and *FSHR* is hypothesized to be the result of WGD before the emergence of Gnathostomata [76]. Our analysis of the molecular phylogeny of vertebrate GpHRs concurs with this notion.

However, by examining the syntenic relationships between the three GpHR subfamilies and the subsequent phylogeny of the flanking *NRXN* genes, we find that *LHCGR* and *FSHR* are tandemly arranged within Tetrapoda. Given that each gene is a derivative of WGD, this colocalization would have occurred before the separation of the Sarcopterygii from the Actinopterygii (~450 mya) (Supplemental Fig. S8). The *NRXN*

analysis reveals that Vertebrata have retained not only complete gene complements of these synaptic proteins but also the propensity for these loci to generate intrachromosomal duplicates. Whereas the physical maps revealed reduced conservation of the syntenic *lhcrba* loci in zebrafish, the alignment synteny showed that this appears to be a rearrangement function. Hence, all teleostean *lhcrb* genes are localized on the b paralogon, suggesting that different species all retain the *lhcrb* type. An alternative scenario would be the translocation of *lhcrb* to the b paralogon. However, such translocations must have occurred randomly throughout teleost evolution, even within closely related Pleuronectiformes. The same problem exists for alternatively retained tandem duplicates. Both scenarios require the rapid degradation of the sister gene. A parsimonious explanation could be interallelic gene conversion (Supplemental Fig. S8); however, the low homology between the *lhcrba* and *lhcrbb* receptors seems to favor a duplicate gene scenario. The present findings thus represent a paradox. Whereas the suggested evolution of the piscine *lhcrb* genes is congruent with their syntenic loci, their exon alignments (Supplemental Fig. S9), and the phylogeny of the flanking *NRXN* genes, further studies will be necessary to validate the enigmatic heritage of piscine *GpHR* genes.

The primary structure of sole *Fshra* and *Lhcrba* show the common structural features among members of the GpHR

family of receptors. However, some important differences are observed when comparing sole Fshra to the FSHRs and LHCGRs of other vertebrates and teleosts. The most prominent structural difference is the inclusion of an extra β -sheet barrel (β 3b) in the interacting domain of the LBD of sole Fshra. The extra β -sheet barrel explains why sole Fshra retains 11 LRRs compared to 10 LRRs in sole Lhcgrba. We found that β 3b is encoded by an additional exon that is specific to the Acanthomorpha. Lower Teleostei and Tetrapoda lack this exon. Whereas splice variants of the pleurinectiform *fshr* have previously been demonstrated [26], none matches the specific locus of the extra β 3b LRR. By wrapping the sole Fshra amino acid sequence to the crystallographically resolved structure of human FSHR [49], we noted that acanthomorph species have potentially evolved duplicate binding sites for their cognate hormones. The significance of this finding is not yet clear, but it can be postulated that additional binding sites within the interaction domain of the exposed receptor surface could have implications for the selectivity and/or affinity of the cognate hormone. We find that unlike mammalian FSHR, which responds exclusively to FSH β [77], sole Fshra responds to both sbFshsc and sbLhsc when expressed in *X. laevis* oocytes. The use of this surrogate system demonstrated that both sole *fshra* and *lhcgrba* encode functional receptors, because the level of intracellular cAMP increased in Fshra- and Lhcgrba-expressing oocytes when exposed to hCG and recombinant piscine Fsh and Lh in a dose-dependent manner. We thus conclude that the sole Fshra may be not selective for its cognate ligand. The endocrine promiscuity of teleost Fshra has also been found in Atlantic salmon [23], North African catfish [78, 79], and zebrafish [80]. Contrary to these reports, however, is our previous observation that European sea bass Fshra was specifically stimulated by bovine FSH [25]. It therefore remains to be established whether such cross-reactions found for the Senegalese sole and other teleosts are purely pharmacological. Indeed, it was recently shown in Atlantic salmon that only ovulatory Lh levels can cross-activate the Fshra; therefore, homologous ligand receptor activation most likely prevails [23]. It is noteworthy, however, that the vertebrate Fsh β chain, which confers biological activity, has reduced sequence conservation compared to its counterpart LH β [7]. The increased complexity of the Acanthomorph Fshra proteins may partly explain the adaptive evolution of the ligand.

Unlike the structural divergence of sole Fshra, we find that sole Lhcgrba has maintained the overall conformation of vertebrate LHCGRs. Sole Lhcgrba also displays greater ligand-specificity compared to Fshra. By contrast, Fsh has been reported to activate Atlantic halibut Lhcgrbb and rainbow trout Lhcgrba [22, 27]. However, Sambroni et al. [22] discussed that rainbow trout Lhcgrba responds only to supraphysiological doses of Fsh, such that trout Lhcgrba most likely has a strong preference for Lh. In our system, sole Lhcgrba was activated by sbFshsc, but only at high doses (1000 ng/ml). This concentration is never encountered in fish plasma, and it probably reflects a pharmacological effect of the hormone. Furthermore, European sea bass Lhcgrba can be activated by bovine FSH but not by endogenous Fsh [25]. Our observations are thus in agreement with those in other teleosts, in which Lhcgrb responds preferentially to Lh whereas Fshra can be activated by either Fsh or Lh [17, 78]. The selectivity of Senegalese sole gonadotropin receptors, however, remains to be conclusively determined in future studies by using purified or recombinant homologous gonadotropins.

To determine whether the Senegalese sole GpHRs confer specific developmental functions, we examined the level of

fshra and *lhcgrba* expression in different adult tissues by qPCR. As expected, we found high expression level of both receptors in the gonads (ovary and testis). However, we also observed a weak expression of *fshra* in the gills, pituitary, and muscle, whereas *lhcgrba* was apparently gonad-specific. Extragonadal expression of *fshra* and *lhcgrb*, such as in gills, brain, kidney, spleen, and heart, has been reported in other teleosts [14, 18, 21, 25, 26] as well as in mammals [81], but the role of the gonadotropin receptors in these tissues remains unclear. Our data also show that *fshra* and *lhcgrba* transcripts were more abundant in the testis than in the ovary, an observation also noted in Atlantic salmon [23] and Japanese eel [13].

The reproductive cycle of Senegalese sole is characterized by distinct seasonal variations in gonad development and maturation, with a major spawning period in spring and a secondary period in autumn [82]. Although changes in annual plasma levels of gonadotropins have not yet been determined in this species, ovarian development has been correlated with variations in the circulating concentrations of different sex steroids as well as of the yolk-precursor vitellogenin [70, 83, 84]. In summer, when plasma levels of testosterone and estradiol are low, the ovary exclusively contains oocytes at the primary growth stage. Oocytes are recruited relatively rapidly into vitellogenesis in February and March, coinciding with the increase of plasma testosterone, estradiol, and vitellogenin. Meiotic maturation of a population of late vitellogenic oocytes is observed in spring (April and May), and at this time, a slight elevation in plasma levels of the maturation-inducing steroid 17 α ,20 β -dihydroxy-4-pregnen-3-one has been detected [70]. Some vitellogenic oocytes often fail to enter into vitellogenesis and become atretic, later being digested and phagocytosed. This process is increased after the spawning season (June). In the present study, we found that the two *gphrs* were differentially expressed in the Senegalese sole at both the ovarian and the follicular level. The expression of *fshra* was closely associated with vitellogenesis, because its expression level increased significantly when the follicles were recruited from the primary growth stage and continued to rise throughout vitellogenesis. However, with the completion of vitellogenesis, its expression level declined during oocyte maturation. In contrast, the expression of *lhcgrba* became evident much later than that of *fshra* and reached its peak level during the late vitellogenic stage, suggesting its role in the induction of oocyte maturation and/or ovulation. The observation that in isolated mature ovarian follicles, *lhcgrba* expression is very low when compared to that in vitellogenic follicles indicates that in the mature ovary, the increased *lhcgrba* transcripts come from follicles at late vitellogenesis. Although we are still lacking information about the circulating levels of Fsh and Lh in Senegalese sole, these observations agree with those reported for other teleosts with group-synchronous ovaries [18, 24, 25, 27, 85], and they seem to support the concept proposed in salmonids for the roles of Fsh and Lh during the ovarian cycle [8, 11].

In the semicyclic testis of Senegalese sole, a high number of Spd, together with some production of Spz, is maintained throughout the year [42, 71]. During the spawning season, however, the Spd number slightly diminishes as the Spz number increases. In the present experiments, we found that the expression of *fshra* and *lhcgrba* in the testis peaks when spermatogenesis is stimulated in winter [42], as evidenced by the increase in the number of SgB and Spc. These observations are consistent with the elevated androgen plasma levels and relative expression of *fshb*, *lhb*, and *cga* subunit transcripts in the pituitary gland during the same period [42]. During the

spawning season, *fshra* mRNA expression in testis diminished to a level corresponding with that found in the resting period (summer), whereas the *lhcrba* transcripts were reduced but maintained a level higher than that in summer. It is not known yet whether the increased *fshra* and *lhcrba* expression in winter results from the proliferation of Sertoli and Leydig cells in the testis or from the up-regulation of the expression of these transcripts in these cells. Nevertheless, the data suggest that both gonadotropin receptors are important for spermatogenesis in Senegalese sole and that *Lhcrba* may play a role at the later stages and/or during spermiation, as proposed for salmonids [37, 38].

We noted some discrepancies, however, concerning the cellular localization of *fshra* and *lhcrba* in the sole testis when compared to other fish species [40, 41, 86]. In the present study, we detected *fshra* transcripts exclusively in the cytoplasm of Sertoli cells surrounding SgA and early SgB, whereas *lhcrba* was found in Leydig cells. Therefore, in Senegalese sole, the specific expression pattern of gonadotropin receptors would fit with the mammalian model in which FSHR and LHCRG are restricted to Sertoli and Leydig cells, respectively. However, in other teleosts, such as the North African catfish and Japanese eel, *Fshra* is also expressed in Leydig cells [40, 41]. In some teleosts, *Fsh* shows strong steroidogenic potency [37, 40, 87], and based on the observations reported in catfish and eel, it could be explained by a direct action of *Fsh* through the *Fshra* of Leydig cells. In the present study, we did not find *fshra* expression in the steroidogenic Leydig cells, but we did find that sole *Fshra* can be activated by both hCG and LH. This suggests that Lh might act on Sertoli cells during the spermiating period, stimulating spermatogenesis and thus allowing a constant production of Spd. It remains to be determined, however, whether *Fsh* in Senegalese sole exerts any steroidogenic action in the testis, as shown in other fish.

An interesting observation during the present study was the detection of strong *lhcrba* expression in Spd. Expression of functional LHCRG has been reported in human sperm [88], but to our knowledge, the present study is the first time that *lhcr* expression has been found in teleost Spd. It would be intriguing to know whether this is a specific feature of teleosts with a semicyclic, asynchronous type of spermatogenesis, in which spermiogenesis occurs gradually, in successive batches, almost year-round. It is tempting to speculate that in Senegalese sole, Lh might regulate the elongation of Spd and transition to Spz, because this event occurs solely via the LHCRG pathway in mammals [31]. This type of regulation would allow the recruitment of successive batches of Spd into spermiogenesis. It is unknown, however, whether *lhcrba* expression in Spd changes during the reproductive cycle; therefore, this hypothesis must be investigated further.

In conclusion, the present study has characterized the *Fshra* and *Lhcrba* of the Pleuronectiform Senegalese sole, for which temporal expression patterns in gonads are consistent with their established roles during fish gametogenesis. As in other teleosts, we found single *fshra* and *lhcrba* transcripts in this species; however, phylogenetic and syntenic analyses revealed that Teleostei retain a *fshra*-type gene of common descent but have evolved alternatively coded *lhcrb*-type genes throughout the crown clade. In addition, Senegalese sole shows an extra LRR (β 3b barrel) located in the interacting domain of the *Fshra*, which arose through exon duplication and appears to be a unique feature of acanthomorph *Fshrs*. As in some other species, sole *Fshra* can be activated by both *Fsh* and Lh, but *fshra* is apparently expressed exclusively in Sertoli cells. In contrast, sole *Lhcrba* seems to be selective for Lh and is

expressed in Leydig cells but most notably in Spds, which may suggest an additional role of this receptor during the transformation of Spd into Spz. How sole *Fshra* and *Lhcrba* are activated by the two gonadotropins *in vivo* as well as the specificity of the ligand-receptor interactions, however, remain to be addressed in further studies. The availability of homologous recombinant gonadotropins in the future will facilitate these studies and provide essential information to unravel the hormonal control of gametogenesis in Senegalese sole and, possibly, in other teleosts with a semicyclic type of spermatogenesis.

REFERENCES

1. Kleinau G, Krause G. Thyrotropin and homologous glycoprotein hormone receptors: structural and functional aspects of extracellular signaling mechanisms. *Endocr Rev* 2009; 30:133–151.
2. Pierce JG, Parsons TF. Glycoprotein hormones: structure and function. *Ann Rev Biochem* 1981; 50:465–495.
3. Park JI, Semyonov J, Chang CL, Hsu SY. Conservation of the heterodimeric glycoprotein hormone subunit family proteins and the LGR signaling system from nematodes to humans. *Endocrine* 2005; 26: 267–276.
4. Kawauchi H, Sower SA. The dawn and evolution of hormones in the adenohipophysis. *Gen Comp Endocrinol* 2006; 148:3–14.
5. Yan L, Swanson P, Dickhoff WW. A two-receptor model for salmon gonadotropins (GTH I and GTH II). *Biol Reprod* 1992; 47:418–427.
6. Quérat B, Arai Y, Henry A, Akama Y, Longhurst TJ, Joss JM. Pituitary glycoprotein hormone beta subunits in the Australian lungfish and estimation of the relative evolution rate of these subunits within vertebrates. *Biol Reprod* 2004; 70:356–363.
7. Levavi-Sivan B, Bogerd J, Mañanós EL, Gómez A, Lareyre JJ. Perspectives on fish gonadotropins. *Gen Comp Endocrinol* 2010; 165: 412–437.
8. Swanson P, Suzuki K, Kawauchi H, Dickhoff WW. Isolation and characterization of two coho salmon gonadotropins, GTH I and GTH II. *Biol Reprod* 1991; 44:29–38.
9. Miwa S, Yan L, Swanson P. Localization of two gonadotropin receptors in the salmon gonad by *in vitro* ligand autoradiography. *Biol Reprod* 1994; 50:629–642.
10. Planas JV, Swanson P. Maturation-associated changes in the response of the salmon testis to the steroidogenic actions of gonadotropins (GTH I and GTH II) *in vitro*. *Biol Reprod* 1995; 52:697–704.
11. Swanson P, Dittman A. Pituitary gonadotropins and their receptors in fish. In: Kawshima S, Kikuyama S (eds.), *Advances in Comparative Endocrinology*. Bologna, Italy: Monduzzi Editore; 1997:841–856.
12. Kagawa H, Tanaka H, Okuzawa K, Kobayashi M. GTH II but not GTH I induces final maturation and the development of maturational competence of oocytes of red seabream *in vitro*. *Gen Comp Endocrinol* 1998; 112:80–88.
13. Jeng SR, Yueh WS, Chen GR, Lee YH, Dufour S, Chang CF. Differential expression and regulation of gonadotropins and their receptors in the Japanese eel, *Anguilla japonica*. *Gen Comp Endocrinol* 2007; 154:161–173.
14. Kumar RS, Ijiri S, Trant JM. Molecular biology of channel catfish gonadotropin receptors: 1. Cloning of a functional luteinizing hormone receptor and preovulatory induction of gene expression. *Biol Reprod* 2001; 64:1010–1018.
15. Kumar RS, Ijiri S, Trant JM. Molecular biology of the channel catfish gonadotropin receptors: 2. Complementary DNA cloning, functional expression, and seasonal gene expression of the follicle-stimulating hormone receptor. *Biol Reprod* 2001; 65:710–717.
16. Laan M, Richmond H, He C, Campbell RK. Zebrafish as a model for vertebrate reproduction: characterization of the first functional zebrafish (*Danio rerio*) gonadotropin receptor. *Gen Comp Endocrinol* 2002; 125: 349–364.
17. Vischer HF, Bogerd J. Cloning and functional characterization of a gonadal luteinizing hormone receptor complementary DNA from the African catfish (*Clarias gariepinus*). *Biol Reprod* 2003; 68:262–271.
18. Kwok HF, So WK, Wang Y, Ge W. Zebrafish gonadotropins and their receptors: I. Cloning and characterization of zebrafish follicle-stimulating hormone and luteinizing hormone receptors—evidence for their distinct functions in follicle development. *Biol Reprod* 2005; 72:1370–1381.
19. Oba Y, Hirai T, Yoshiura Y, Yoshikuni M, Kawauchi H, Nagahama Y. The duality of fish gonadotropin receptors: cloning and functional

- characterization of a second gonadotropin receptor cDNA expressed in the ovary and testis of amago salmon (*Oncorhynchus rhodurus*). *Biochem Biophys Res Commun* 1999; 265:366–371.
20. Oba Y, Hirai T, Yoshiura Y, Yoshikuni M, Kawauchi H, Nagahama Y. Cloning, functional characterization, and expression of a gonadotropin receptor cDNA in the ovary and testis of amago salmon (*Oncorhynchus rhodurus*). *Biochem Biophys Res Commun* 1999; 263:584–590.
 21. Maugars G, Schmitz M. Molecular cloning and characterization of FSH and LH receptors in Atlantic salmon (*Salmo salar* L.). *Gen Comp Endocrinol* 2006; 149:108–117.
 22. Sambroni E, Le Gac F, Breton B, Lareyre JJ. Functional specificity of the rainbow trout (*Oncorhynchus mykiss*) gonadotropin receptors as assayed in a mammalian cell line. *J Endocrinol* 2007; 195:213–228.
 23. Andersson E, Nijenhuis W, Male R, Swanson P, Bogerd J, Taranger GL, Schulz RW. Pharmacological characterization, localization and quantification of expression of gonadotropin receptors in Atlantic salmon (*Salmo salar* L.) ovaries. *Gen Comp Endocrinol* 2009; 163:329–339.
 24. Mittelholzer C, Andersson E, Taranger GL, Consten D, Hirai T, Senthilkumaran B, Nagahama Y, Norberg B. Molecular characterization and quantification of the gonadotropin receptors FSH-R and LH-R from Atlantic cod (*Gadus morhua*). *Gen Comp Endocrinol* 2009; 160:47–58.
 25. Rocha A, Gómez A, Zanuy S, Cerdà-Reverter JM, Carrillo M. Molecular characterization of two sea bass gonadotropin receptors: cDNA cloning, expression analysis, and functional activity. *Mol Cell Endocrinol* 2007; 272:63–76.
 26. Kobayashi T, Andersen Ø. The gonadotropin receptors FSH-R and LH-R of Atlantic halibut (*Hippoglossus hippoglossus*). 1: Isolation of multiple transcripts encoding full-length and truncated variants of FSH-R. *Gen Comp Endocrinol* 2008; 156:584–594.
 27. Kobayashi T, Pakarinen P, Torgersen J, Huhtaniemi I, Andersen Ø. The gonadotropin receptors FSH-R and LH-R of Atlantic halibut (*Hippoglossus hippoglossus*). 2. Differential follicle expression and asynchronous oogenesis. *Gen Comp Endocrinol* 2008; 156:595–602.
 28. An KW, Lee KY, Yun SG, Choi CY. Molecular characterization of gonadotropin subunits and gonadotropin receptors in black porgy, *Acanthopagrus schlegelii*: effects of estradiol-17beta on mRNA expression profiles. *Comp Biochem Physiol B Biochem Mol Biol* 2009; 152:177–188.
 29. Vassart G, Pardo L, Costagliola S. A molecular dissection of the glycoprotein hormone receptors. *Trends Biochem Sci* 2004; 29:119–126.
 30. Bogerd J. Ligand-selective determinants in gonadotropin receptors. *Mol Cell Endocrinol* 2007; 260–262:144–152.
 31. Allan CM, García A, Spaliviero J, Zhang FP, Jimenez M, Huhtaniemi I, Handelsman DJ. Complete Sertoli cell proliferation induced by follicle-stimulating hormone (FSH) independently of luteinizing hormone activity: evidence from genetic models of isolated FSH action. *Endocrinology* 2004; 145:1587–1593.
 32. Zhang C, Shimada K, Saito N, Kansaku N. Expression of messenger ribonucleic acids of luteinizing hormone and follicle-stimulating hormone receptors in granulosa and theca layers of chicken preovulatory follicles. *Gen Comp Endocrinol* 1997; 105:402–409.
 33. Hillier SG. Gonadotropin control of ovarian follicular growth and development. *Mol Cell Endocrinol* 2001; 179:39–46.
 34. Saint-Dizier M, Malandain E, Thoumire S, Remy B, Chastant-Maillard S. Expression of follicle-stimulating hormone and luteinizing hormone receptors during follicular growth in the domestic cat ovary. *Mol Reprod Dev* 2007; 74:989–996.
 35. Yaron Z, Gur G, Melamed P, Rosenfeld H, Elizur A, Levavi-Sivan B. Regulation of fish gonadotropins. *Int Rev Cytol* 2003; 225:131–185.
 36. Nagahama Y, Yamashita M. Regulation of oocyte maturation in fish. *Dev Growth Differ* 2008; 50:S195–S219.
 37. Schulz RW, Miura T. Spermatogenesis and its endocrine regulation. *Fish Physiol Biochem* 2002; 26:43–56.
 38. Miura T, Miura C. Molecular control mechanisms of fish spermatogenesis. *Fish Physiol Biochem* 2003; 28:181–186.
 39. Swanson P, Dickey JT, Campbell B. Biochemistry and physiology of fish gonadotropins. *Fish Physiol Biochem* 2003; 28:53–59.
 40. Ohta T, Miyake H, Miura C, Kamei H, Aida K, Miura T. Follicle-stimulating hormone induces spermatogenesis mediated by androgen production in Japanese eel, *Anguilla japonica*. *Biol Reprod* 2007; 77:970–977.
 41. García-López A, Bogerd J, Granneman JC, van Dijk W, Trant JM, Taranger GL, Schulz RW. Leydig cells express follicle-stimulating hormone receptors in African catfish. *Endocrinology* 2009; 150:357–365.
 42. Cerdà J, Chauvigné F, Agulleiro MJ, Marin E, Halm S, Martínez-Rodríguez G, Prat F. Molecular cloning of Senegalese sole (*Solea senegalensis*) follicle-stimulating hormone and luteinizing hormone subunits and expression pattern during spermatogenesis. *Gen Comp Endocrinol* 2008; 156:470–481.
 43. Agulleiro MJ, Anguis V, Cañavate JP, Martínez-Rodríguez G, Mylonas CC, Cerdà J. Induction of spawning of captive-reared Senegal sole (*Solea senegalensis*) using different administration methods for gonadotropin-releasing hormone agonist. *Aquaculture* 2006; 257:511–524.
 44. Agulleiro MJ, Scott AP, Duncan N, Mylonas CC, Cerdà J. Treatment of GnRHa-implanted Senegalese sole (*Solea senegalensis*) with 11-ketoandrostenedione stimulates spermatogenesis and increases sperm motility. *Comp Biochem Physiol A Mol Integr Physiol* 2007; 147:885–892.
 45. Fabra M, Cerdà J. Ovarian cysteine proteinases in the teleost *Fundulus heteroclitus*: molecular cloning and gene expression during vitellogenesis and oocyte maturation. *Mol Reprod Dev* 2004; 67:282–294.
 46. Finn RD, Tate J, Mistry J, Coghill PC, Sammut JS, Hotz HR, Ceric G, Forslund K, Eddy SR, Sonnhammer EL, Bateman A. The Pfam protein families database. *Nucleic Acid Res* 2008; Database Issue 36:D281–D288.
 47. Bendtsen JD, Nielsen H, von Heijne G, Brunak S. Improved prediction of signal peptides: SignalP 3.0. *J Mol Biol* 2004; 340:783–795.
 48. Krogh A, Larsson B, von Heijne G, Sonnhammer ELL. Predicting transmembrane protein topology with a hidden markov model: application to complete genomes. *J Mol Biol* 2001; 305:567–580.
 49. Fan QR, Hendrickson WA. Structure of human follicle-stimulating hormone in complex with its receptor. *Nature* 2005; 433:269–277.
 50. Finn RN. Vertebrate yolk complexes and the functional implications of phosphatins and other subdomains in vitellogenins. *Biol Reprod* 2007; 76:936–948.
 51. Finn RN, Kristoffersen BA. Vitellogenin gene duplication in relation to the “3R hypothesis”: correlation to the pelagic egg and the oceanic radiation of teleosts. *PLoS ONE* 2007; 2:e169.
 52. Notredame C, Higgins DG, Heringa J. T-Coffee: a novel method for fast and accurate multiple sequence alignment. *J Mol Biol* 2000; 302:205–217.
 53. Ronquist F, Huelsenbeck JP. Mr Bayes 3: Bayesian phylogenetic inference under mixed models. *Bioinformatics* 2003; 19:1572–1574.
 54. Zmasek CM, Eddy SR. ATV: display and manipulation of annotated phylogenetic trees. *Bioinformatics* 2001; 17:383–384.
 55. Deen PM, Verdijk MA, Knoers NV, Wieringa B, Monnens LA, van Os CH, van Oost BA. Requirement of human renal water channel aquaporin-2 for vasopressin-dependent concentration of urine. *Science* 1994; 264:92–95.
 56. Schatz SM, Kerschbaumer RJ, Gerstenbauer G, Kral M, Dorner F, Scheiflinger F. Higher expression of Fab antibody fragments in a CHO cell line at reduced temperature. *Biotechnol Bioeng* 2003; 84:433–438.
 57. Cerdà J, Mercadé J, Lozano JJ, Manchado M, Tingaud-Sequeira A, Astola A, Infante C, Halm S, Viñas J, Castellana B, Asensio E, Cañavate P, et al. Genomic resources for a commercial flatfish, the Senegalese sole (*Solea senegalensis*): EST sequencing, oligo microarray design, and development of the Soleamold bioinformatic platform. *BMC Genomics* 2008; 9:508.
 58. Manchado M, Infante C, Asensio E, Canavate JP. Differential gene expression and dependence on thyroid hormones of two glyceraldehyde-3-phosphate dehydrogenases in the flatfish Senegalese sole (*Solea senegalensis* Kaup). *Gene* 2007; 400:1–8.
 59. Kobe B, Kajava AV. The leucine-rich repeat as a protein recognition motif. *Curr Opin Struct Biol* 2001; 11:725–732.
 60. Murakami M, Kouyama T. Crystal structure of squid rhodopsin. *Nature* 2008; 453:363–368.
 61. Gether U. Uncovering molecular mechanisms involved in activation of G protein-coupled receptors. *Endocr Rev* 2000; 21:90–113.
 62. Taylor JS, Braasch I, Frickey T, Meyer A, Van de Peer Y. Genome duplication, a trait shared by 22 000 species of ray-finned fish. *Genome Res* 2003; 13:382–390.
 63. Vandepoel K, De Vos W, Taylor JS, Meyer A, Van de Peer Y. Major events in the genome evolution of vertebrates: paranome age and size differ considerably between ray-finned fishes and land vertebrates. *Proc Natl Acad Sci U S A* 2004; 101:1638–1643.
 64. Rissone A, Monopoli M, Beltrame M, Bussolini F, Cotelli F, Arese M. Comparative genome analysis of the neurexin gene family in *Danio rerio*: insights into their functions and evolution. *Mol Biol Evol* 2007; 24:236–252.
 65. Finn RN, Kolarevic J, Kongshaug H, Nilsen F. Evolution and differential expression of a vertebrate vitellogenin gene cluster. *BMC Evol Biol* 2009; 9:2.
 66. Soreq H. The biosynthesis of biologically active proteins in mRNA-microinjected *Xenopus* oocytes. *CRC Crit Rev Biochem* 1985; 18:199–238.
 67. Gudermann T, Nichols C, Levy FO, Birnbaumer M, Birnbaumer L. Ca²⁺ mobilization by the LH receptor expressed in *Xenopus* oocytes

- independent of 3',5'-cyclic adenosine monophosphate formation: evidence for parallel activation of two signaling pathways. *Mol Endocrinol* 1992; 6: 272–278.
68. Tingaud-Sequeira A, Chauvigné F, Lozano J, Agulleiro MJ, Asensio E, Cerdà J. New insights into molecular pathways associated with flatfish ovarian development and atresia revealed by transcriptional analysis. *BMC Genomics* 2009; 10:434.
 69. García-López A, Martínez-Rodríguez G, Sarasquete C. Male reproductive system in Senegalese sole *Solea senegalensis* (Kaup): anatomy, histology and histochemistry. *Histol Histopathol* 2005; 20:1179–1189.
 70. García-López A, Anguis V, Couto E, Canario AVM, Cañavate JP, Sarasquete C, Martínez-Rodríguez G. Noninvasive assessment of reproductive status and cycle of sex steroid levels in a captive wild broodstock of Senegalese sole *Solea senegalensis* (Kaup). *Aquaculture* 2006; 254:583–593.
 71. García-López A, Fernández-Pasquier V, Couto E, Canario AVM, Sarasquete C, Martínez-Rodríguez G. Testicular development and plasma sex steroid levels in cultured male Senegalese sole *Solea senegalensis* Kaup. *Gen Comp Endocrinol* 2006; 147:343–351.
 72. Yu S, Hsu T. New insights into the evolution of the relaxin–LGR signaling system. *Trends Endocrinol Metab* 2003; 14:303–309.
 73. Freamat M, Kawauchi H, Nozaki M, Sower SA. Identification and cloning of a glycoprotein hormone receptor from sea lamprey, *Petromyzon marinus*. *J Mol Endocrinol* 2006; 37:135–146.
 74. Freamat M, Sower SA. A sea lamprey glycoprotein hormone receptor similar with gnathostome thyrotropin hormone receptor. *J Mol Endocrinol* 2008; 41:219–228.
 75. Hsu SY, Nakabayashi K, Bhalla A. Evolution of glycoprotein hormone subunit genes in bilateral metazoa: identification of two novel human glycoprotein hormone subunit family genes, GPA2 and GPB5. *Mol Endocrinol* 2002; 16:1538–1551.
 76. Oba Y, Hirai T, Yoshiura Y, Yoshikuni M, Kawauchi H, Nagahama Y. Fish gonadotropin and thyrotropin receptors: the evolution of glycoprotein hormone receptors in vertebrates. *Comp Biochem Physiol B Biochem Mol Biol* 2001; 129:441–448.
 77. Hearn MT, Gomme PT. Molecular architecture and biorecognition processes of the cystine knot protein superfamily: part I. The glycoprotein hormones. *J Mol Recognit* 2000; 13:223–278.
 78. Vischer HF, Granneman JC, Linskens MH, Schulz RW, Bogerd J. Both recombinant African catfish LH and FSH are able to activate the African catfish FSH receptor. *J Mol Endocrinol* 2003; 31:133–140.
 79. Vischer HF, Granneman JC, Koelink PJ, Marques RB, Bogerd J. Identification of a luteinizing hormone-selective determinant in the exodomain of a follicle-stimulating hormone receptor. *Gen Comp Endocrinol* 2008; 156:490–498.
 80. So WK, Kwok HF, Ge W. Zebrafish gonadotropins and their receptors: II. Cloning and characterization of zebrafish follicle-stimulating hormone and luteinizing hormone subunits—their spatial-temporal expression patterns and receptor specificity. *Biol Reprod* 2005; 72:1382–1396.
 81. Rao CV. An overview of the past, present, and future of nongonadal LH/hCG actions in reproductive biology and medicine. *Semin Reprod Med* 2001; 19:7–17.
 82. Anguis V, Cañavate JP. Spawning of captive Senegal sole (*Solea senegalensis*) under a naturally fluctuating temperature regime. *Aquaculture* 2005; 243:133–145.
 83. García-López A, Couto E, Canario AV, Sarasquete C, Martínez-Rodríguez G. Ovarian development and plasma sex steroid levels in cultured female Senegalese sole *Solea senegalensis*. *Comp Biochem Physiol A Mol Integr Physiol* 2007; 146:342–354.
 84. Guzmán JM, Norberg B, Ramos J, Mylonas CC, Mañanós EL. Vitellogenin, steroid plasma levels and spawning performance of cultured female Senegalese sole (*Solea senegalensis*). *Gen Comp Endocrinol* 2008; 156:285–297.
 85. Rocha A, Zanuy S, Carrillo M, Gómez A. Seasonal changes in gonadal expression of gonadotropin receptors, steroidogenic acute regulatory protein and steroidogenic enzymes in the European sea bass. *Gen Comp Endocrinol* 2009; 162:265–275.
 86. Schulz RW, Vischer HF, Cavaco JE, Santos EM, Tyler CR, Goos HJ, Bogerd J. Gonadotropins, their receptors, and the regulation of testicular functions in fish. *Comp Biochem Physiol B Biochem Mol Biol* 2001; 129: 407–417.
 87. Aizen J, Kasuto H, Golan M, Zakay H, Levavi-Sivan B. Tilapia follicle-stimulating hormone (FSH): immunochemistry, stimulation by gonadotropin-releasing hormone, and effect of biologically active recombinant FSH on steroid secretion. *Biol Reprod* 2007; 76:692–700.
 88. Eblen A, Bao S, Lei ZM, Nakajima ST, Rao CV. The presence of functional luteinizing hormone/chorionic gonadotropin receptors in human sperm. *J Clin Endocrinol Metab* 2001; 86:2643–2648.